Fat Fractionation by Distillation

Master's thesis

Eetu Tuohi

Process and Systems Engineering Laboratory

Faculty of Science and Engineering

Åbo Akademi University

Supervisor: Prof. Ron Zevenhoven

Instructors: M.Sc. Artturi Ropponen, M.Sc. Riitta Kujala

Turku, Finland. February 2020.

ÅBO AKADEMI UNIVERSITY – FACULTY OF SCIENCE AND ENGINEERING
Abstract for Master’s Thesis

Title: Fat Fractionation by Distillation	**Date**: 20.2.2020
Author: Eetu Tuohi	**Subject**: Process Design and Systems Engineering
Supervisor: Prof. Ron Zevenhoven	**Instructors**: M.Sc. Riitta Kujala, M.Sc. Artturi Ropponen

Abstract:

The demand for renewable fuels and chemicals is growing, but at the same time, discussion about the use of edible raw materials in the production has intensified. Waste-based fats and oils are cheaper and their consumption is generally more acceptable than edible feedstock’s. They are, however, more challenging to process as their composition and availability varies substantially. Waste-based fats and oils may contain, for example, solid particles, chlorides and volatile organic compounds (VOCs). The literature part of this thesis reviews some of the edible and non-edible feedstocks, suitable pre-processing methods and distillation techniques for the fat and oil feedstocks.

The applied part of the thesis studies the separation of free fatty acids (FFA) and glycerides by distillation from a waste-based fat feedstock. As a result, two distillation concepts were developed and simulated in Aspen Plus. The constructed base case feed had a feed FFA content of 65%. The distillation column bottom temperature of the concepts was kept below 260 °C in order to avoid the possible thermal decomposition of the fat feedstock. The first concept included a side-stream distillation column with 6 separation stages. The FFA fraction was taken out as a side-stream, the light fraction, including water, VOCs and organochlorides, was drawn as an overhead stream while the glyceride fraction was drawn from the bottom. FFA recovery via the side-stream was 86.2% of the feed’s FFA in the base case simulation. The FFA purity of the side-stream was over 99.99% and the glyceride purity of the bottom stream was 79.5%. 400 kg of steam was injected to the column in order to bring the bottom temperature below 260 °C. The turndown ratio of the column geometry, for this concept, was excellent as the column could be operated with varying feed FFA content between 90 wt.% and 20 wt.%.

The second concept included a pre-flash drum before a simple distillation column with 3 separation stages. The light fraction was separated in the flash drum, the FFA fraction was taken out as an overhead stream while the glycerides were obtained as a bottom stream. The same level of FFA recovery to the overhead stream was achieved with the pre-flash concept as with the side-stream concept. Compared to the side-stream concept, glyceride fraction purity was about the same, but the FFA fraction purity was slightly worse for the pre-flash concept. The energy input requirment of the pre-flash concept was, however, 0.7 MW less than for the side-stream concept due to more effective heat integration. The turndown ratio of the pre-flash concept was worse than the side-stream column concept’s because jet flooding occurred at high feed FFA contents (90% or more) while the bottom temperature rose over 260 °C at low feed FFA content (50% or less). For both concepts, modified Sulzer-Nutter BDH valve trays were chosen as column internals as they resulted in the best performance with respect to column diameter and pressure drop under the deep vacuum conditions used. Lower pressure drop and column diameter are obtainable with structured packings, but these were not selected due to uncertain fouling characteristics of fat feedstock.

Keywords: Distillation, side-stream column, pre-flash drum, Aspen Plus, process simulation	**Pages**: 81

ÅBO AKADEMI – FAKULTETEN FÖR NATURVETENSKAPER OCH TEKNIK
Abstrakten för diplomarbetet

Titel: Destillation av avfallsoljor och -fett	**Datum**: 20.2.2020
Författare: Eetu Tuohi	**Ämne**: Process- och systemteknik
Handledare: Prof. Ron Zevenhoven	**Handledare**: DI Riitta Kujala, DI Artturi Ropponen

Abstrakt:

Efterfrågan på förnybara bränslen och kemikalier växer, men samtidigt motståndet mot användning av ätbara fetter och oljor som råvaror har ökat. Avfallsbaserade fetter och oljor erbjuder på ett billigare och generellt mer acceptablare alternativ. Problemet är dock att de oätbara avfallsoljorna innehåller orenheter så som klorider (organiska och inorganiska), lättflyktiga organiska föreningar (VOC:er), vatten och fasta partiklar som försvårar deras behandling. I den här avhandlingen presenteras några ätbara och oätbara råvaror, lämpliga förbehandlingstekniker och destillationsmetoder.

I den praktiska delen av den här avhandlingen, separation av de fria fettsyrorna (FFA) och glyceriderna från avfallsoljorna med destillation behandlas. Två destillationskoncept utvecklades och simulerades i Aspen Plus. Ett konstruerat inflöde hade 65 % FFA-innehåll och bottentemperatur av destillationskolonner hölls under 260 °C för att undvika möjlig termisk nedbrytning av inflödet. Det första destillationskonceptet innehöll en sidoströmskolonn med 6 bottnar. FFA-fraktionen erhölls som en sidoström, den lätta fraktionen, som innehöll vatten, VOCer, organoklorider och lätt FFA erhölls från kolonnens topp medan glyceriderna erhölls som en bottenström. Den uppnådda FFA-fraktionen blev 86,2 % av det konstruerade inflödets FFA. FFA-Renheten av sidoströmmen var över 99,99 % och glycerid-renheten hos bottenströmmen var 79,5 %. 400 kg ånga injekterades till kolonnen för att behålla bottentemperaturen under 260 °C. Destillationskolonnen kunde drivas med ett varierande FFA-innehåll hos inflödet mellan 90 vikt-% och 20 vikt-%.

Det andra konceptet innehöll en flash-behållare före en destillationskolonn med 3 bottnar. Den lätta fraktionen separerades i flash-behållaren, FFA-fraktionen erhölls från kolonnens topp och glyceriderna erhölls som en bottenström. En lika stor FFA-fraktion uppnåddes som i det första konceptet. Glycerid-renheten var lika bra men FFA-renheten var litet sämre jämfört med sidoströmskolonn-konceptet. Konceptet med flash-behållaren krävde 0,7 MW mindre energi på grund av en effektivare värme-integrering jämfört med sidoströmskolonn-konceptet. Konceptet med flash-behållaren drabbades av översvämningen vid höga FFA-halter hos inflödet (90 % eller mera) och bottentemperaturen steg över 260 °C vid låga FFA-halter hos inflödet (50 % eller mindre). Båda koncepten kördes under i ett djupt vakuum (10 mbar). Modifierade Sulzer-Nutter BDH ventilbottnar valdes över de andra simulerade bottentyperna eftersom de presterade bäst. En packning valdes inte på grund av oron att inflödet skulle vara för smutsigt. Sulzer Mellapack strukturerad packning hade annars varit det bästa alternativet då tryckförlustet och den resulterande diametern skulle vara mycket mindre än hos de valda bottnarna.

Nyckelord: Destillation, sidoströmskolonn, flash-behållare, Aspen Plus, process simulation	**Antal sidor**: 81

Svensk sammanfattning

Syftet med det här diplomarbetet är att presentera några möjligheter för separation av fria fettsyror (FFA) och glycerider från avfallsoljor med hjälp av destillation. De mest lovande destillationskoncepten simulerades i Aspen Plus V10.

Växtbaserade oljor består i huvudsak av triacylglyceroler (kallas triglycerider), men innehåller också diglycerider, monoglycerider och fria fettsyror. Triglycerider är estrar av tre fettsyramolekyler och en glycerolmolekyl. Vid höga temperaturer bryts triglyceriderna ner till diglycerider, monoglycerider och eventuellt till glycerol och fria fettsyror.

De växtbaserade oljorna kan delas i två grupper på basen av deras ätlighet. Användningen av ätbara växtbaserade oljor som råvara till andra ändamål än matprodukter har träffat hårt motstånd. EU har satt en strikt agenda med målet att förhindra användningen av palmolja i alla bränslen senast år 2030. På grund av pressen från EU, klimatfrågor och matbrist, har industrin börjat söka efter nya råvaror för förnybara bränslen. Oätbara råvaror omfattar använda stekoljor, avfallsoljor från palmoljeindustrin och djurfett. Fördelar med användningen av avfallsoljor som råvara för bränsleproduktion är att de är mycket billigare än ätbara, bearbetade oljor. Problemet är dock att de oätbara avfallsoljorna innehåller en hel del orenheter så som klorider (organiska och inorganiska), fosfor, metaller, lättflyktiga organiska föreningar (VOC:er), vatten och fasta partiklar som försvårar deras behandling.

Det rekommenderas att avfallsoljorna behandlas före destillation för att undvika problem med korrosion och täppning i destillationskolonnen. De fasta partiklarna kan till exempel filtreras bort genom pressfiltrering. Man kan också använda centrifug för separation av de fasta partiklarna. De inorganiska kloriderna, som orsakar korrosion under en destillationsprocess, kan avlägsnas genom att tvätta råvaran med vatten och applicera elektrisk spänning för att separera de salta vattendropparna.

En destillationsprocess baseras på skillnader i kokpunkter mellan olika ämnen i en blandning. Den enklaste formen av destillation i processindustrin kan utföras i en flash-behållare där de lättaste (mest flyktiga) ämnena förångas från inflödet. De tunga ämnena med högre kokpunkt fås som en bottenström. Flash-destillationen ger ofta en dålig separation vilket leder till att en destillationskolonn med flera bottnar behövs.

I en destillationskolonn förångas processmediet på botten med hjälp av en återkokare och kyls på toppen med hjälp av en kondensor. Kolonnen innehåller antingen bottnar

eller en kolonnpackning vars uppgift är att garantera en bra kontakt mellan den stigande ångan och det fallande kondensatet. Ju fler bottnar eller kolonnpackningar man har, desto effektivare är separationen.

Ett inflöde för Aspen Plus-simuleringar konstruerades med hjälp av litteraturreferenser som beskriver avfallsoljornas sammansättningar. Inflödet som användes i grundsimuleringar hade högt FFA-innehåll på 65 massprocent. Flödet hade också en hög vattenhalt (2,2 %) och relativt hög VOC- (382,9 ppm) samt organisk kloridhalt (60 ppm). Meningen med hög FFA-, vatten-, VOC-, och kloridhalt var att imitera sönderfallen fett eller olja.

Två olika destillationskoncept utvecklades för att separera de fria fettsyrorna och glyceriderna från avfallsoljorna. Konceptet som utvecklades mest innehöll bara en enda destillationskolonn där både lätta och tunga substanser separerades från de fria fettsyrorna. Det här betyder att FFA togs ut från mitten av kolonnen som en sidoström. Sidoströmmen var väldigt ren och dess sammansättning var 99,99 % FFA. Bottenströmmens glycerid-renhet var 79,5 %. Toppgaserna innehöll mest vattenånga, ungefär alla lättflyktiga organiska föreningar samt en del av de organiska kloriderna. Bottenströmmen innehöll tri-, di-, och monoglycerider, tunga fria fettsyror samt 66,6 % av de organiska kloriderna.

I det andra konceptet ingick en flash-behållare före destillationskolonnen. Meningen med detta var att förenkla separationen av FFA och de tyngre glyceridkomponenterna. Då den största delen av de lätta komponenterna separerades före destillationskolonnen, tog man FFA-strömmen från kolonntoppen. Renheten hos FFA-strömmen var inte lika bra eftersom med flash-behållaren lyckades inte att separera bort varken allt vatten, klorider eller de lättflyktiga organiska föreningarna. Glycerid-renheten av bottenströmmen var lika bra som i det andra konceptet.

Sidoströmskolonnen drevs under ett högt vakuum (10 mbar) för att sänka bottentemperaturen och således undvika nedbrytning och polymerisation av inflödet. Vakuumet produceras med hjälp av ångejektorer. I kolonnen finns det också en ångkoppling vars funktion är att kunna köra ånga in i kolonnen för att sänka bottentemperaturen.

Olika bottentyper testades i simuleringarna men Sulzer-Nutter BDP-ventilbottnar presterade bäst. Tryckförlusten och kolonndiametern var de lägsta med de valda bottnarna. Trycket spelar en stor roll i vakuumdestillation eftersom bottentemperaturen växer då tryckförlusten blir större och det måste undvikas. Olika kolonnpackningar testades också men i praktiken kan de antagligen inte användas på grund av risken för kraftig försmutsning. Kolonnpackningarna tål inte heller fasta partiklar eller processdriftförändringar.

En viktig avsikt var att undersöka om samma kolonn kan användas för olika typer av inflöden. Detta undersöktes genom att ändra på FFA-halten i råvaran. Resultaten visade att det går att driva destillationskolonnen mellan 90 % och 10 % FFA men att det blir mycket dyrare när FFA-halten minskar. Detta orsakas av flera saker. Då råvaran innehåller mindre mängder FFA, blir inflödet tyngre vilket leder till en högre kokpunkt. Det betyder att bottentemperaturen stiger och vattenångan måste injekteras till kolonnen eller utflödena måste minskas. Kolonnen kan också torka upp om vätskeflödet i den minskar för mycket. Det här leder till att man måste cirkulera processämnen inom kolonnen bara för att undvika torkningen. Bortsett från problemen med låga FFA-halter visar simuleringarna lovande resultat för konceptet med sidoströmskolonnen som kunde utvecklas vidare i samarbete med en leverantör.

Preface

This master's thesis, which is written for Neste Engineering Solutions Ltd (NES), is the last step of my journey to graduate from Åbo Akademi University.

Thank you Raisa Vermasvuori and Johanna Vaittinen for the opportunity to write this thesis about a very interesting and pleasant subject for NES. I am also forever grateful for Stefan Karlsson for giving me the first chance to prove myself at NES.

Thank you Professor Ron Zevenhoven, M.Sc. Riitta Kujala and M.Sc. Artturi Ropponen for putting in countless hours of commenting and helping me to improve my thesis and tirelessly guiding me through this project. Also, huge thanks to the whole Åbo Akademi University personnel for always finding the time to help me with the study-related subjects.

Last but not least, thank you to my dear, indispensable parents, family and friends for your support through this journey and for staying by my side, even during my darkest moments.

In Porvoo, 10th of February 2020

Eetu Tuohi

Table of Contents

Abbreviations

3-MCPD	3-monochloro-1,2-propanediol	ppb	Parts per billion
BG	Brown grease	ppm	Parts per million
BOD	Biological oxygen demand	ptb	Parts per thousand barrels
CAPEX	Capital expenditures	PTG	Polymerized triglycerides
CF	Chicken fat	RBD	Refined, bleached, deodorized
COD	Chemical oxygen demand	SDE	simultaneous steam distillation and extraction
CWG	Choice white grease	SMILES	Simplified molecular-input line-entry system
FAME	Fatty acid methyl ester	SPD	Short-path distillation
FFA	Free fatty acid	SPHE	Spiral plate heat exchanger
GHG	Greenhouse gas	SPO	Sludge palm oil
HVO	Hydrotreated vegetable oil	STHE	Shell and tube exchanger
LCA	Life cycle assessment	UCO	Used cooking oil
MESH	material balance, phase equilibrium, summation condition, heat balance	UNIFAC	UNIQUAC Functional-group Activity Coefficients
MIU	Moisture, insoluble, unsaponifiables	UNIQUAC	universal quasichemical
NRTL	Nationally Recognized Testing Laboratory	WCO	Waste cooking oil
OPEX	Operating expenditures	VLE	vapor-liquid equilibrium
PHE	Gasketed plate heat exchanger	VOC	Volatile organic compound
POME	Palm oil mill effluent	YG	Yellow grease

Notation

C	Cost
C_p	Heat capacity
Eff_i^v	Vaporization efficiency
$Eff_{i,j}^M$	Murphree efficiency
$F\ factor$	Factor for column diameter inspection
h	Column height
$K_{i,j}$	Equilibrium K value of component i on stage j
L	Column height
m	Mass
N_T	Number of stages in Aspen Plus
P	Heating/cooling duty
T	Temperature
V_{max}	Maximum vapor velocity
$x_{i,j}$	Liquid mole fraction of component i on stage j
$y_{i,j}$	Vapor mole fraction of component i on stage j
ρv	Vapor density
μ	Efficiency

1 Introduction

Due to the growing demand for renewable fuels and chemicals, usage of more demanding feedstocks in the biofuel and chemical industry has become more and more important. According to Owen *et al.* [1], the volume of consumed fossil oil was three times larger than the volume of discovered crude oil in 2007. Shafiee *et al.* [2] presented a new modified Klass model which computed depletion times for the main fossil fuels. The fossil oil depletion time was calculated to be around 35 years for resources known today. BP's statistical review of world energy in 2018 and the global reserves to production ratio shows that the oil reserves will last for 50 years of current production [3]. Though it is impossible to forecast an accurate date for oil reserves depletion, they will not last forever and thus the consumption of bio-based alternatives needs to grow. The other natural driving factors for the usage of bio-based fuels are related to concerns over the global warming. The life cycle assessment (LCA) studies have shown that the greenhouse gas (GHG) emissions from renewable diesel (hydrotreated vegetable oil, HVO) are more than 80% lower compared to petroleum diesel and about 40% lower than the traditional first generation biodiesel [4]. In addition to lower environmental impacts, renewable diesel is superior even to traditional diesel with its higher heating value and lower cloud point. The traditional FAME-type biodiesel on the contrary, is not considered as an equivalent alternative to fossil-based diesel. [4]

Biodiesel is manufactured by transesterification of triglycerides and methanol in the presence of a catalyst, while renewable diesel is produced through a catalytic reaction including hydroprocessing of triglycerides [5]. Both renewable diesel and biodiesel can be manufactured from renewable feedstocks such as vegetable oils, animal fat and waste oils and fats from food industry. The most popular vegetable oil feedstocks are rapeseed, soybean and palm oil. As mentioned before, bio-based diesel fuels produce less GHG emissions compared to fossil oil-based diesel. [4] There are, however, a couple of major drawbacks in using renewable oils as a feedstock for diesel: the high price of refined vegetable oil and the fact that the feedstock could be used as food [6]. One way to tackle both of these problems is to use waste fats and oils as a feedstock. There are already several companies taking care of the collection of waste oils and fats from restaurants and other food-related businesses. Other waste and residual streams originate, for example, from palm oil industry including palm fatty acid distillates (by-product) and palm oil mill effluent (process waste). The prices of waste cooking oil and virgin canola oil were compared in 2000 by Zhang *et al.* [7]. The price of waste cooking oil was defined to 200 $/ton while the reported price of virgin canola oil was 500 $/ton. The inflation adjusted annual average price of crude oil during the year 2000 was 293 $/ton and 423 $/ton in 2018 [8].

While the usage of waste feedstocks, such as used cooking oil and palm oil mill effluent, might sound tempting due to the low price and other environmental aspects, they present their challenges. The waste feedstock properties tend to vary considerably depending on the source from where they are collected from and the way they were processed. Moreover, it is not lucrative to attempt to transform the waste feedstocks directly into products as they may contain problematic amounts of impurities, including organochlorides, volatile organic compounds, solid particles, sulfur, metals and moisture. [9-18]

The focus of this master's thesis is to investigate different distillation concepts that can be applied in fractionation of waste fat or oil feedstocks. The most promising concepts are simulated in Aspen Plus and an economical evaluation is performed in order to find the most feasible technology. The fatty acid compositions and other constituents of potential waste feedstocks are examined in detail in the literature part. Other pre-processing methods such as desalting, filtering and settling are also briefly discussed. The thesis is divided in to a literature part and an applied part. The literature part describes lipids, edible and non-edible feedstocks, different pre-treatment processes, distillation concepts and distillation simulation using Aspen Plus. The applied part describes the used methods, results and economical evaluation.

LITERATURE PART

2 Renewable feedstocks

Renewable fat and oil feedstocks for biofuel and –chemical production can be categorized as edible and non-edible. The usage of edible feedstocks for purposes such as fuel production is facing much of controversy. For example, the EU has set a 2030 deadline to phase out the use of crude palm oil in fuels, even if it is certified as sustainable [19]. The edible feedstocks are, however, briefly discussed as many of the non-edible feedstocks are residuals originating from the usage or production of edible oils. Non-edible feedstocks also include some oil-yielding plants, such as jatropha and soapnut, which are not covered in this thesis [20]. Non-edible feedstocks that are covered, are used cooking oil, palm oil mill effluent (not to be confused with the much debated refined palm oil) and animal fats.

2.1 Fatty acids and triglycerides

Natural oils and fats consist mostly of triglycerides. Typical, detailed compositions of different feedstocks are reviewed in the later chapters. Triglycerides consist of fatty acids. Gunstone *et al.* [21] make four general statements that define the nature of fatty acids well. There are quite a few exceptions, but the main principles are expressed below:

1. Most natural fatty acids, both saturated and unsaturated, are straight-chain compounds with an even number of carbon atoms in their molecules. The carbon chain length is commonly between 12 and 22 atoms.
2. Most acids with one unsaturated center are usually olefinic compounds with cis (Z) configuration with the double bond in a limited number of preferred positions, commonly at n-9 (nine carbon atoms from the carboxyl group).
3. Polyunsaturated acids are mainly polyolefinic with a methylene-interrupted arrangement of double bonds having cis (Z) configuration. The double bonds are separated from each other by one CH_2 group (1, 4 pattern of unsaturation).
4. Fatty acids rarely have other functional groups than carboxyl group and various types of unsaturation. [21]

It has been estimated that 8 acids account for 97% in the total production of vegetable oils and they are presented in Table 2.1 by Gunstone *et al.* [21].

Table 2.1 The most common fatty acids in produced vegetable oils [21]

Common name of fatty acid	Explanation of structure	percent of total production
Lauric	C_{12}	4
Myristic	C_{14}	2
Palmitic	C_{16}	11
Stearic	C_{18}	4
Oleic	C_{18}, double bond at C_9	34
Linoleic	C_{18}, double bonds at C_9 and C_{12}	34
A-linoleic	C_{18}, double bonds at C_9, C_{12} and C_{15}	5
Eruric	C_{22}, double bond at C_9 calculated from the methyl end	3

Fatty acids seldom occur in their free state (free fatty acid, FFA), but usually as esters and sometimes as amides. Esters contain acid and alcohol components and the most common alcohol present in lipids is glycerol (propane-1,2,3-triol). The majority of lipids are triglycerides (triacylglycerols), but mono- and diacylglycerols may also be present as minor components. Triglycerides are fully acylated derivatives of glycerol. It is unusual for a natural triglyceride to have only one type of acid. Usually, two or three different acids are present and the variation of triglycerides rises rapidly with the number of acids present in the fatty acid pool. [21] For example palm oil consists mostly of POP (30.2 area-%), POO (23.3 area-%), PLP (9.2 area-%), PLO (8.9 area-%), PPP (6.7 area-%) and POS (6.7 area-%). Here P stands for palmitic, O for oleic, L for linoleic and S for stearic acid. The combination of letters details which fatty acids are present in the triglyceride [22]. Palmitic acid and tripalmitin (PPP) are illustrated in Figure 2.1.

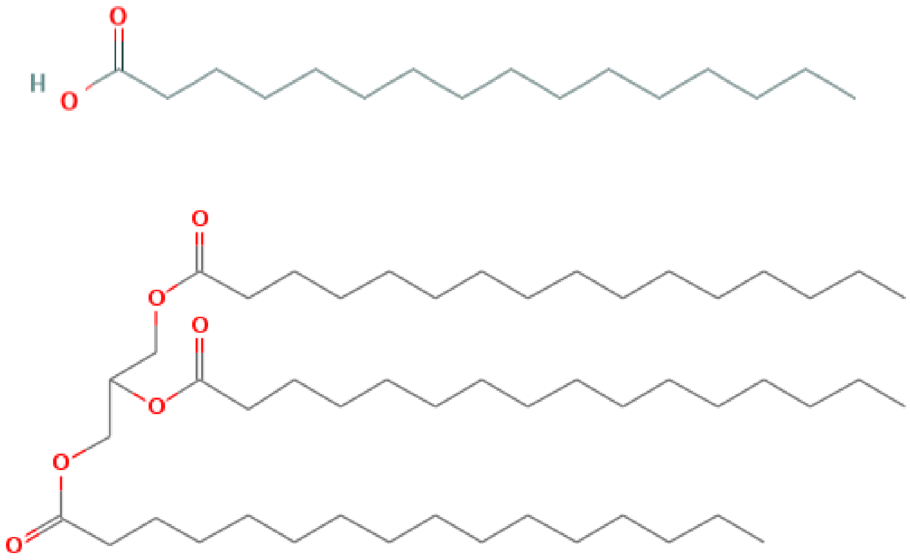

Figure 2.1 Structures of palmitic acid and tripalmitin (PPP) [23, 24]

The properties of different fatty acids and triglycerides play a vital role when modelling fat distillation, which exploits the differences in boiling points or volatilities between the components in the mixture [25]. Unfortunately, there are drastic differences in the literature values for boiling points of fatty acids and triglycerides depending on the source of information and calculation method. For example estimations with the Gani group contribution method resulted in radically different predicted normal boiling point values for fatty acids compared to the Joback group contribution method in a study conducted by Santander *et al.* [26]. In experimental measurements, one reason for the significant differences of boiling points could be due to the thermal degradation of triglycerides at higher temperatures. Wallek *et al.* reported that the measurements of the triglycerides' boiling points turned out to be challenging mainly because of potential decomposition of the substances around and above the normal boiling point. [27] Palanisamy *et al.* [28] studied thermal degradation of triglycerides and showed that at 350 °C and 5 bar, 58% of rapeseed oil's triglycerides were decomposed to oxygenate, light and heavy hydrocarbons, CO and CO_2. At 1 bar, 36% of triglycerides were decomposed. Navar [29] presented results about hydrolysis of triglycerides heated at 200 °C for 3 hours. The results showed that 18% of lauric, 14% of palmitic and 16.6% of oleic acid were hydrolyzed. The study also showed that shorter chains and acids with unsaturation give an increased rate to hydrolysis. In practice, triglycerides can be thermally decomposed through diglycerides to monoglycerides and to glycerols and free fatty acids [29]. This means that the experimental boiling point measurement may be difficult and differences in literature values of boiling points depend on the laboratory methods or mathematical estimation models. Specific gravity, melting point and boiling point of some common fatty acids and triglycerides are presented in Table 2.2 by Southard *et al.* [30]. The boiling points for corresponding substances in the Aspen Plus V11 PURE37 databank are included in the table for comparison.

Table 2.2 Properties of some fatty acids and triglycerides [30]

Substance	Specific gravity	melting point (°C)	boiling point (°C)	Boiling point in Aspen Plus V11 (°C)
Oleic acid	0.854	14	285-286	359.9
Palmitic acid	0.849	63-64	271.5	351
Linoleic acid	0.903	-9.5	229-230	354.9
Tripalmitate (PPP)	0.866	65.1	310-320	602.9
Trioleate (OOO)	0.915	-4	240	846.9

In addition to thermal degradation of triglycerides in high temperatures, thermal oxidation of unsaturated hydrocarbon chains causes polymerization. Triglyceride oligomers such as dimers and 6rimmers have a higher molecule weight than triglyceride monomers. Accumulation of polymers leads to undesirable phenomena such as color deepening and viscosity increase of the vegetable oils. When oxygen is absent, dimerization or polymerization is achieved by linkage of –C-C- to form dimers or polymers without extra oxygen atom. In the presence of oxygen, polymerization can also occur by the linkage of –C-O-C- and –C-O-O-C-. [31] Sánchez-Muniz *et al.* [32], Tasioula-Margari *et al.* [33] and Takeoka *et al.* [34] analyzed the polar content of different used cooking oils. The polar compounds include dimeric fatty acids, triglyceride monohydroperoxides, polymerized triglycerides (PTG), cyclic fatty acid monomers and aldehydic triglycerides [35]. The results of Takeoka *et al.* [34] are presented in Figure 2.2.

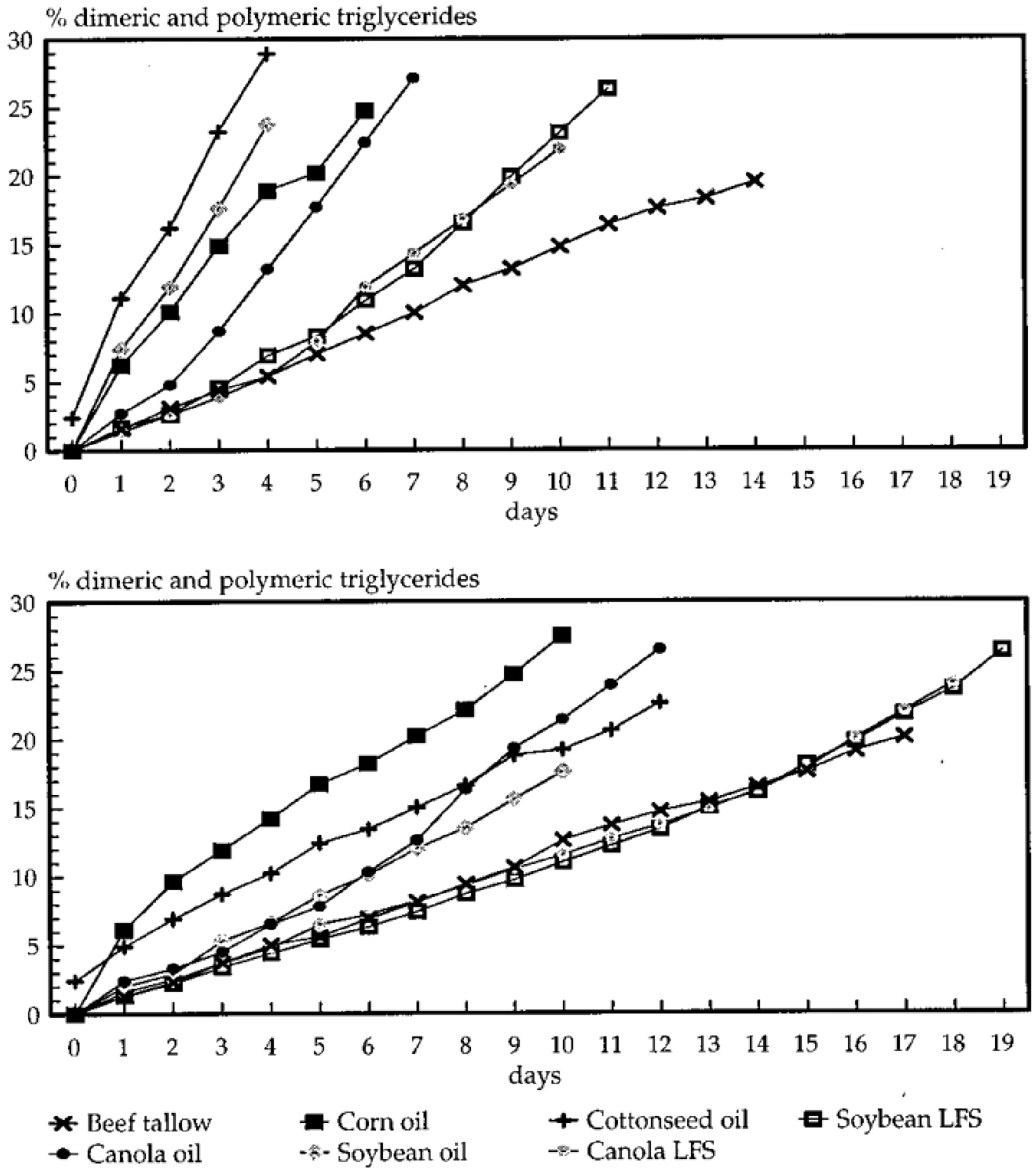

Figure 2.2 Amount of dimeric and polymeric triglycerides of different oils after heating 8 h/day at 190 °C (bottom) and 204 °C (top) [34]

The polymerization products can be separated according to size and polarity, but the molecular structures and cross-linkages of the complex polymeric species are still widely unknown. However, a study conducted by Bonetti *et al.* [36] suggests that cross-linking in vegetable oil polymerization occurs through ester groups. The revelation was possible through a simplified study using oleic acid without a glycerol body. The study does not detail how an ester bond would be established between triglycerides. [36] Choe *et al.* [37] describe –C-O-C- and –C-O-O-C- linkages between the triglyceride dimers and polymers with them having a molar mass of 692-1600 g/mol.

2.2 Edible feedstocks

In 2016, the world FAME-based biodiesel production reached 32.18 billion liters. The EU region was the biggest producer with an annual production of 13.68 billion liters while the USA came second producing 10.94 billion liters. The largest volume feedstock worldwide in 2013 was rapeseed (canola) oil covering 68% of the used feedstock. Soybean oil (15%) took the second place which is also the main biodiesel feedstock in the USA. Palm oil covered 6% of the total usage being the third largest volume biodiesel feedstock. [38] Within the group of vegetable oils, the chosen feedstock varies geographically based on its availability and usually the locally most abundant vegetable oil is chosen. This is not only because an ample, steady supply of feedstock is needed but also because the feedstock can constitute the major part of the total biodiesel production costs. [39] Typical fatty acid compositions (wt.%) of the three largest biodiesel feedstock vegetable oils are presented in Table 2.3 by Gunstone *et al.* [21].

Table 2.3 Typical fatty acid compositions of rapeseed, soybean and palm oil [21]

Vegetable oil	16:0 (palmitic)	18:1 (Oleic)	18:2 (Linoleic)	Other (incl., %)
Rapeseed	4	56	26	14 (18:3, 10)
Soybean	11	22	53	14 (18:3, 8)
Palm	44	40	10	6

Rapeseed oil grows in cooler agricultural regions including northern Europe, China, Canada and Indian subcontinent. The crude rapeseed oil fatty acids consist mostly of oleic acid (56%) and it is rich in phospholipids (~ 3.5%). [21] Ghazani *et al.* [40] also characterized rapeseed oil. According to their study, crude rapeseed oil's FFA content is 0.3 – 1.2% and it is high in phosphorus (300 – 500 ppm). It is also unique due to its high chlorophyll content (4-30 ppm). If the chlorophyll content is too high, it has a negative impact on oil's oxidative stability (a measure of oil's resistance to oxidation) [40].

Soybean has become an important oil crop during the last 50 years even though the oil is actually a byproduct in the manufacturing of high-protein animal feed. Approximately half of the world's soybean is grown in the USA, followed by Brazil, Argentina and China. Soybean oil's fatty acids consist mostly of linoleic acid (53%) and it is also high in phospholipids (3.2%). [21] The typical FFA content of crude soybean oil is 0.3 – 0.7% according to Pryde [41].

The oil palm grows in tropical regions of Asia, Africa and America. The oil palm tree is the most producing oil crop yielding as much as 5-7 tons oil/ hectare on well-managed plantations. The fatty acids mostly consist of palmitic (44%) and oleic (40%). [21] The phospholipid content of crude palm oil is around 5 – 130 ppm and the FFA content is under 5% [42].

2.3 Used cooking oil

Used cooking oils (UCO), also referred to waste cooking oils (WCO), are primarily bio-based fat and oil waste from restaurants, households and food industry that have been used for cooking or food preparation and are no longer suitable for consumption. An accurate number for global UCO production is not available, but it has been estimated that more than 15 million tons is produced annually. The referred estimate does not consider India, Africa and South America, therefore, the real number is probably much larger. [43]

As the cost of vegetable oil plays a crucial role in the total manufacturing economics of biodiesel, used cooking oil has become an attractive feedstock alternative. The costs of vegetable oils can cover up to 75% of the total costs of biodiesel manufacturing. The high price of edible vegetable oils has led the total production costs of biodiesel to be 1.5 times higher than the conventional fossil oil-based diesel. [44, 45, 7]

UCO was previously added to animal feed until the EU banned it in 2002 because of animal health concerns and the subsequent circulation back in to the food chain. The disposal of UCO also includes problems, as discharging it into drains or sewers leads to blockages, odor, vermin problems and possible watercourse pollution. UCO has nevertheless shown promise as a possible feedstock for biofuels and it is largely available worldwide. [43]

Before the actual cooking process, the frying oils are very clean as they go through a careful manufacturing process. Nearly all the oils used in cooking are so-called RBD oils which means that they are refined, bleached and deodorized [46]. Heating of RBD oils results in chemical reactions which produce unwanted reaction products and the rest of the impurities originate from the fried foodstuffs [45].

Kulkarni *et al.* [45] described three types of reactions occurring in vegetable oil when exposed to frying: thermolysis, oxidation and hydrolysis. Thermolytic reactions occur when triglycerides containing saturated fatty acids are heated at high temperature (180 °C) in the absence of oxygen. Mainly series of alkanes, 1-alkenes, lower fatty acids, symmetric ketones, oxopropyl esters, propene and propane diesters and diacylglycerols are formed as products of heating. Acrolein, CO and CO_2 are also formed. In the oxidative reactions, unsaturated fatty acids react with molecular oxygen via a free radical mechanism. Primarily hydroperoxides are formed during the reaction and may further form isometric hydroperoxides which contain conjugated diene groups. The decomposition of the O-O bonds of hydroperoxides produce alkoxy radicals which may gain loose hydrogen atoms and furthermore form the hydroxyl or keto derivatives. When the alkoxy radicals decompose, aldehydes, hydrocarbons, semialdehydes and acids are formed. In hydrolytic reactions, steam which is formed during the food preparation causes the hydrolysis of triglycerides. As a result, free fatty acids FFA, glycerol, monoglycerides and diglycerides are formed. [45]

The exact composition of UCO can vary heavily based on its origin. A chemical analysis of a UCO, which was collected from restaurants inside the Cincinnatti Zoo and Botanical Garden and analyzed by Chai *et al.* [9], is presented in Table 2.4. The 5 wt.% FFA content is low compared to other samples found in the literature. The FFA content of a sample collected from a restaurant in Las Cruces by Patil *et al.* [10] was 8.71 wt.%. Wang *et al.* [11] reported a really high FFA value of 37.96 wt.% in a sample collected from restaurants in China. The water, phosphorus and sulfur contents of the sample from the Cincinnatti Zoo were on an acceptable level and the feedstock could have been employed, for example, to FAME biodiesel production [47, 9]

Table 2.4 Chemical analysis of UCO used in esterification pretreatment study [9]

Test	Result
Free fatty acid	5.0 wt.%
Triglycerides	89.6 ± 1.0 wt.%
Diglycerides	5.2 ± 0.2 wt.%
Monoglycerides	1.4 ± 0.2 wt.%
Density	0.920 g/ml
Water	0.23 v/v%
Sediment	~ 0.5 v/v%
MIU (moisture, insoluble, unsaponifiables)	< 1 wt.%
Phosphorus	9.0 ppm
Sulfur	5.6 ppm

The intense odor of used cooking oils is related to their chemical composition, particularly to the volatile fraction. Mannu *et al.* [48] analyzed used cooking oil by headspace solid-phase microextraction coupled with gas chromatography (HS-SPME GC/MS) and managed to identify a total of 46 volatile organic compounds (VOCs). Several different classes of compounds were detected: aldehydes, alcohols, ketones, hydrocarbons, and acids. Takeoka *et al.* [49] isolated UCO samples from a food-processing plant by atmospheric SDE (simultaneous steam distillation and extraction) and identified 140 different compounds. The major constituents were 1-pentanol, hexanal, furfuryl alcohol, €-2-heptenal, 5-methylfurfural, 1-octen-3-ol, octanal, 2-pentylfuran, €-2-octenal, nonanal, €-2-nonenal, and hexadecanoic acid. Wu *et al.* [50] studied the changes of volatile organic compounds in soybean oils generated by deep frying the oil for one hour and stored at 55 °C. A total of 47 different compounds were identified after which the sample was stored in air for 26 weeks at 55 °C. The study showed that the amount of VOCs rose from 164 ppm to 862 ppm due to oxidation. [50]

2.4 Palm oil mill effluent

Palm oil production has turned to a noteworthy agriculture-based industry in Malaysia and Indonesia during the recent decades. The number of processing mills has elevated from 10 operated mills in 1960 to 410 mills in 2008. In Malaysia alone, at least 44 million tons of palm oil mill effluent (POME), also known as sludge palm oil (SPO), was produced as a by-product of refinement. Most palm oil mills have adopted a ponding system of the mill effluent. The high production rate of 44 million tons most likely refers to these oily water ponds. Four general types of treatment systems have been employed and they consist of waste stabilization ponds, activated sludge systems, closed anaerobic digester and land application system. [51]

Although POME is classified as a nontoxic waste, it has a very high chemical oxygen demand (COD) of 16000-100000 mg/l and biochemical oxygen demand (BOD) (10250-43750 mg/l), which creates a serious threat to aquatic life [51, 52]. The high quantities of total solids (~40500 mg/l) also contain great amounts of nutrients which could trigger an algae bloom [51]. POME has a high nitrogen content ranging from 200 to 500 mg/l and high content of amino acids and phosphorus as well as varying amount of FFA [52]. Suwanno *et al.* [12] experimented with an FFA content of 27.7 wt.% while Hayaan *et al.* [13,14] used POME with 23.2 wt.% and 22.3 wt.% in their experiments. The reported phosphorus contents vary between 8.7 ppm and 11.1 ppm [53, 13, 14]. Habib *et al.* [54] quantified a total of 23 different minerals in raw palm oil mill effluent. The fatty acid composition was highly similar to crude palm oil illustrated in Table 2.3. Fatty acids of POME were mostly palmitic (42.8 wt.%) and oleic (39.6 wt.%) including also 10 wt.% of linoleic [13]. Similar compositions were also produced by Suwanno *et al.* [12] although the fatty acid distribution also seems to vary. Habib *et al.* [54] reported high myristic acid content (12.7 wt.%) and lower palmitic acid content (22.5 wt.%). The reported moisture contents of POME varied from 0.87 wt.% to as high as 6.99 wt.% [12-14, 54].

The focus of treating POME as waste has started leaning towards transforming POME into more useful assets. Foo *et al.* [52] introduced methods to utilize POME, for example, in hydrogen, fertilizers, carotene, biofuel and microbiological chemical production. Several authors have also described methods for FAME biodiesel production from the palm oil mill effluent [12-14].

2.5 Animal fats

Animal fats are primarily derived as by-products from meat animal processing plants and rendering processes. Animal fats and oils are also generated by the fish and leather industry. The main animal fats include tallow from processing cattle, lard and choice white grease from swine processing, and poultry fat from the processing of chicken, turkey or other birds. [55]

Animal by-products can be divided into three different risk classes. Different categories give different rules on how the by-products can be handled and disposed as waste. Materials from all the categories are allowed to be used for biodiesel and renewable diesel production. Only category 3 materials may be used in animal feed production after an appropriate treatment in approved processing plants. [56]

As the animal fats are a wide category, their fatty acid compositions depend on the origin of the material and vary considerably. Table 2.5 illustrates the fatty acid compositions of some main animal fats. Here YG stands for yellow grease, BG brown grease, CWG choice white grease and CF chicken fat. [55]

Table 2.5 Fatty acid profiles of different animal fats [55]

Fatty acid	Carbon number	YG	BG	CWG	Lard	Tallow	CF
Lauric	C12:0						
Myristic	C14:0	1.0	1.7	1.60	1.4	2.8	
Palmitic	C16:0	14.8	23.8	22.4	25.7	26.0	22.2
Palmitioleic	C16:1	1.5	3.1	3.4	2.8	2.8	8.4
Stearic	C18:0	8.4	12.5	9.2	17.5	17.5	5.1
Oleic	C18:1	47.9	42.4	44.1	41.7	41.7	42.5
Linoleic	C18:2	19.1	12.1	11.9	6.9	6.9	19.3
Linolenic	C18:3	4.7	0.8				1.0
Arachidic	C20:0	2.6		7.4	0.4	0.4	
Eicosenoic	C20:1				1.9	1.9	

3 Pre-processing

Waste feedstocks may contain such high amounts of solids, heavy particles, chlorides and other impurities that their fractionation with distillation as such would not be reasonable [16, 17]. Problems with blocking, fouling and corrosion can be avoided by pre-treating the feedstocks [57-59]. Ways to remove solids, heavy particles and chlorides are described in this chapter. Methods for lowering the raw material FFA content prior to FAME-production are also considered.

3.1 Solid and heavy particles removal

In order to avoid blocking or fouling during the distillation, most of the solid particles in a feed should be removed. Sidibé *et al.* [60] recommend two techniques for filtration of heavy particles, metals and phospholipids from the vegetable oils. The first one is oil decanting, which might take several days or even weeks. The purpose is to let the oil rest so that the heaviest solids can descend by gravity to the bottom of the tank. This is a cost-effective method but takes a lot of time and space. The separation efficiency is not great and a final filtration step is recommended afterwards. Another method is direct filtration, where the oil is pressed through a plate or filter press. The filtration should be carried out between 20 and 60 °C. Low temperature makes direct filtration difficult because of the high viscosity of straight vegetable oils. On the other hand, too high temperatures may enable undesirable particles to pass through the filter. Ideally the filtering medium penetration size should be 10 μm. [60]

For UCO and transesterified UCO (FAME), several different solid/liquid separation methods have been reported in literature [61, 62, 45]. Issariyakul *et al.* [61] used a centrifuge to remove the solids in UCO and added 10 wt.% silica gel to absorb the high amount of water. The silica gel in turn, was removed by vacuum filtration using Whatman filter paper (No. 40 Quantitative). Sudhir *et al.* [62] let their UCO samples to stand for 2-3 days so that the impurities would settle down by gravity. Then the solids were filtered away. Kulkarni *et al.* [45] also report the use of settling and filtration for transesterified UCO.

Some relatively new studies present different filtration methods for POME [15, 16, 63]. Ibrahim *et al.* [15] applied horizontal roughing filter with limestone media in order to reduce the amount of chemical organic demand (COD), NH_3-N, turbidity, color and suspended solids. The optimum reduction was found with the filtration rate of 0.3 m/h where 57.4% of suspended solids were removed. Yunos *et al.* [16] studied ultrafiltration of palm oil mill effluent on different pressures and stirring speeds. The suspended solid content was reduced from 43 ppm to under 25 ppm while the dissolved solids were reduced from 890 ppm to 541 ppm. Zafisah *et al.* [63] also showed that cake filtration can be applied to separate suspended solids from anaerobic POME digestate.

3.2 Dealing with inorganic and organic chlorides

Both fossil- and vegetable-based crude oils contain chlorides that can cause serious corrosion and lead into hazardous situations such as leakages. This means that the feedstocks have to be desalted before further unit operations, such as distillation, occur. The chlorides can be dealt to inorganic and organic chlorides. The typical chloride values of fossil oil vary depending on the source. Nag [64] reports the crude salts to be around 10-20 part per thousand barrels (ptb) (28.5-57.1 ppm), while Nager *et al.* [65] describe that the fossil crude oil contains 3-200 ptb (8.6-570.6 ppm) salts. The crude oil salts consist mostly NaCl (70-75%), $CaCl_2$ (10%) and $MgCl_2$ (10-15%) [66]. Organic chlorides do not occur naturally in crude oil, but are believed to result from contamination such as disposal of chlorinated solvent used in many dewaxing pipelines. Organochlorides break down during fractionation and produce hydrochloric acid, which is extremely corrosive. [67]

The chloride content of vegetable oils is usually not as high as in fossil oils. Inorganic chloride can be found in commercial vegetable oils such as maize (6.31 ppm), sunflower (1.75 ppm), soy (1.87 ppm) and peanut (1.04 ppm) oil [68]. According to Wai Lin *et al.* [69], the chloride content in palm oil varies from 3 to 10 ppm. Nagy *et al.* [70] showed that both inorganic and organic chlorinated substances are present in every stage of palm oil processing and even in the palm fruits themselves before milling. The organochlorides of edible oils are mostly 3-monochloro-1,2-propanediol fatty esters (3-MCPD esters) [70, 71]. Waste cooking oils contain larger amounts of chlorides. A Chinese patent about organic chloride removing methods states that the chloride levels in waste cooking oil can be as high as 20 ppm (mostly organic chlorides) [17]. Another study conducted by Chen *et al.* [18] describing UCO states that their sample contained 5.48 ppm chlorides.

Desalting is a well-known process from the fossil oil refineries which is done to remove salts (inorganic), suspended solids and water before any other unit operations. An electric desalting method is introduced in Figure 3.1. The feed is washed with water at a temperature of 93-149 °C. The amount of wash water ranges from 3 to 10 volume-% and the operating conditions are determined by the specific gravity of the crude oil. The salts dissolve in the wash water and the oil and water phases are separated in a settling vessel. The separation can be done by adding chemicals to break up emulsion or by applying an electrostatic field to coalesce the salt water droplets. Either an AC or DC field may be applied at potentials of 16000-35000 V [72]. A two-stage desalter can achieve lower than 1 ptb (pounds per thousand barrels) (2.9 ppm) salt levels while a one-stage desalter only reaches 1-3 ptb (2.9-8.6ppm) [64]. The water removal efficiency in a two-stage desalter is 99% and 90-95% in a single-stage desalter [72].

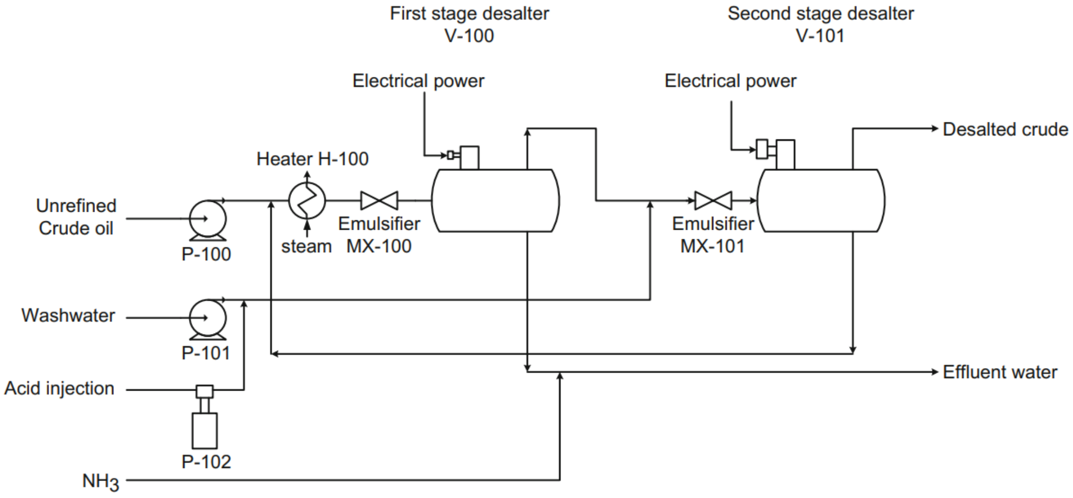

Figure 3.1 A two-stage desalting unit [72]

The organic chlorides are by far harder to handle than the inorganic salts because they cannot be removed from the feedstock by traditional electrical desalting. This means that even if the chloride-levels would be reduced, significant corrosion could still arise [58]. Especially the crude distillation overhead systems are prone to accumulation of the organochlorides [58, 66]. Most refineries do not allow more than 1 ppm organic chlorides in the crude [59]. Following issues have been reported when the organochloride levels have risen unnoticed:

- A series of sudden tube leaks in the crude tower’s overhead heat exchangers.
- Crude tower’s bad operation because of the accumulation of organochlorides in the reflux system.
- Corrosion in the overhead and recirculation system of the fluidized catalytic cracker.
- Damaged stabilizer at the catalytic reforming unit.

- Blockage and corrosion in the hydrogenation reactor. [58, 59]

The simplest countermeasure against corrosion caused by organic chlorides would be to blend contaminated crude oil with non-chlorinated crude oil so that the concentration would not get problematically high [58]. Nag [64] suggests the use of amines or ammonia in the overhead to arrest the corrosion of the overhead. Both Nag [64] and Li *et al.* [58] report that the organic amines have better neutralization and corrosion inhabitation effect than ammonia. Other measures such as the usage of molecular sieves have also been widely discussed in the literature [73, 74]. For vegetable oils, methods for removal of 3-MCPD esters from palm oil at different production stages were discussed by Matthäus *et al.* [71]. A part of organochlorides can be washed away from the raw material even before the actual milling with water and ethanol. In the deodorizing stage, injection of formic acid into the stripping steam prevents formation of 3-MCPD esters. An enzymatic conversion of the organochlorides into glycerol has also been suggested after the deodorization. [71]

3.3 Methods to lower the FFA content prior to FAME production

By-products of frying reactions in UCO can lead to further formation of many undesired components in connection to FAME production. Several authors have mentioned the problems concerning raised FFA and moisture levels of UCO during the transesterification stage of the feedstock [47, 75, 9, 43]. Especially, the transesterification of UCO in the presence of a homogenous base catalyst has reportedly led to undesirable reactions between the free fatty acids and the catalyst. This leads to soap formation, yield loss and increased difficulty in product separation. Freedman *et al.* [47] stated that the feedstock to be employed in alkali-catalyzed transesterification should be substantially anhydrous and have an acid value less than 1. Acid value is defined as the mass of potassium hydroxide (KOH) in milligrams that is needed to neutralize one gram of chemical substance. The acid value can roughly be converted to FFA percent by dividing the acid value with 1.99. [76] Freedman's *et al.* [47] study showed that even 0.3% moisture in the reaction reduced the glycerol yields by consuming catalyst. Alkali catalysts such as NaOH and KOH could be replaced with acid catalysts like sulfuric acid and hydrochloric acid. However, acidic catalysts are often not deployed in commercial transesterification processes, because of the longer reaction times. [77] According to Gui *et al.* [43], the acidic catalysts are also corrosive to equipment. The usual commercial solution is to pretreat UCO or other high FFA content feedstock and then employ the alkali-catalyzed transesterification method. A well-known industrial pretreatment method is an acid-catalyzed esterification to lower the FFA content [9, 78]. Caustic stripping has also been practiced but acid esterification is economically dominant [9]. Even acid-catalyst esterification has its downfall as the additional chemicals raise the total costs. The National Renewable Energy Laboratory (NREL) of the USA recommends the total dosage of 2.25 g methanol and 0.05 g sulfuric acid for every gram of FFA in oil [9]. Diaz-Felix *et al.* [78] stated that the FFA content and the consequential amount of methanol are the main factors affecting the economics of FAME biodiesel production from UCO.

Similar pre-treatment methods have also been employed in POME processing. The studies of Hayaan *et al.* [13, 14] focused on a two-step process. The idea in both studies was to first pretreat the solution by esterification in order to lower the FFA content to under 2%. The pretreated solution was then traditionally converted to biodiesel by transesterification in the presence of alkali catalyst. In the study conducted by Suwanno *et al.* [12], no pretreatment step was taken as the transesterification was directly conducted with a crude lipase acquired from oil palm fruit.

High FFA content is not a problem in production of renewable diesel, which is a great advantage over FAME biodiesel as the range of feedstocks becomes flexible and esterification is not needed. The first step of renewable diesel production is actually the scission of propane from the glycerol backbone of the triglyceride molecules in presence of hydrogen in order to form free fatty acids. [79]

4 Distillation

Distillation units are found all over the chemical industry. It is, for example, the main separation process in crude oil refining. Depending on the complexity and size, there could be 30 or more distillation columns in one refinery [80]. Distillation is a thermal separation process and often considered to be the most important or the main operation in a conventional oil refinery. The process separates fractions in a homogenous mixture based on their boiling point difference or relative volatility. Distillation alone might stand for 40% of a crude oil refinery's energy requirement [64]. In this chapter, the principles of single- and multi-stage distillation are described and different distillation concepts are presented. Deodorization and short-path distillation are special cases of distillation and they are also discussed, because of their implementation in the edible oil industry.

4.1 Flash distillation and pre-flash concepts

When speaking about flash distillation, usually single-stage separation of the gas and liquid phases in a flash drum is meant. However, some multi-stage distillation concepts can also be referred as pre-flash towers, pre-cut columns or pre-flash columns. These concepts are also introduced in this chapter despite the fact that they consist of multiple stages.

Flash distillation is one of the simpler distillation concepts, which can be employed if the vapor pressures of the components differ substantially enough [81]. Different variations of flashing exist and a couple of them are shortly presented here. In Figure 4.1, the pressurized liquid stream is fed to a heater and flashed adiabatically after a valve to a lower pressure. If pressure is lowered below the bubble point pressure of the mixture at the given temperature, the vapor phase is created and separated from the remaining liquid in a flash drum. In Figure 4.2, in the absence of the valve, liquid is partially vaporized in a heater and separated from the liquid in the flash drum without a pressure decrease [82]. Flash units might be placed in series in order to achieve purer components because typically, flashing is not purity-wise the most efficient means of separation [83].

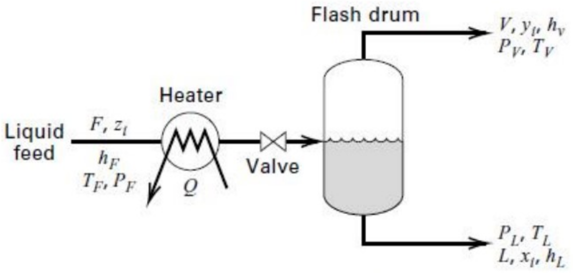

Figure 4.1 Flash distillation including pressure-reducing valve [82]

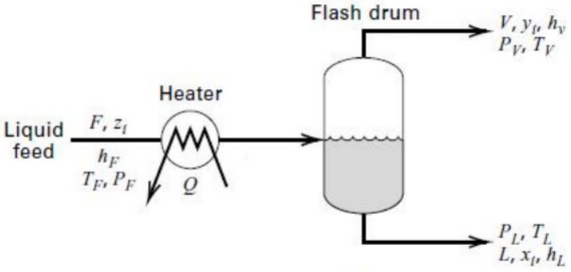

Figure 4.2 Flash distillation without pressure-reducing valve [82]

Flash distillation is commonly used in petroleum industry. Different kinds of pre-flash drum and pre-flash tower configurations can be deployed in the crude distillation unit upstream of the main fractionation column. Their purpose is to vaporize some lighter fractions of crude oil feed. The vaporized feed, if pure enough (pre-flash tower design), can be led directly through the condenser to a stabilizer column. When using a pre-flash drum, the vaporized stream is led past the crude oil preheating train and the furnace directly to the fractionating tower, as seen in Figure 4.3. The benefits of pre-flashing include reduced pressure drop of the furnace, reduced likelihood of crude vaporization at the furnace inlet (flashing) and reduced water content of the crude prior to the last heat exchangers and the furnace. A pre-flash tower is also the best alternative for debottlenecking a crude oil distillation unit's capacity, as it reduces the diameter requirements of the distillation tower and the stabilizer. [64]

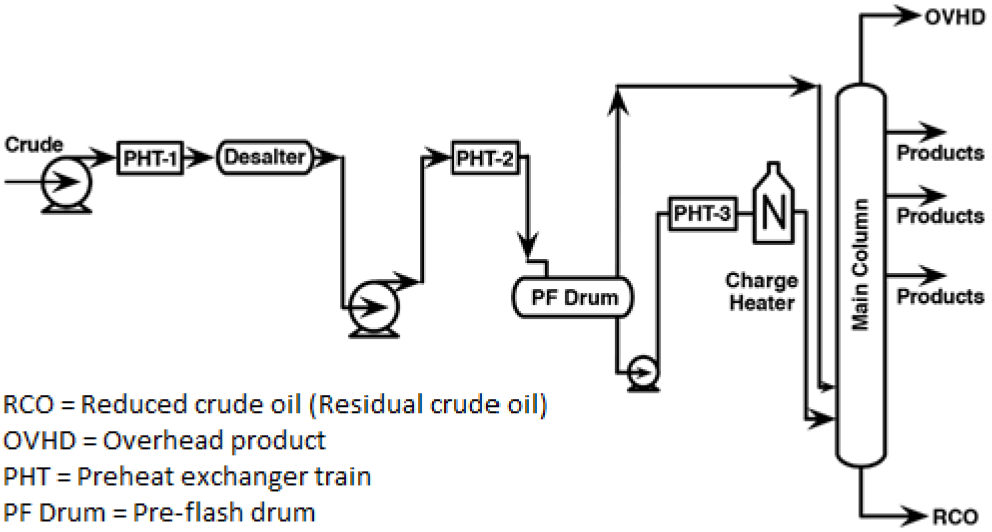

Figure 4.3 Crude distillation unit including a pre-flash (PF) drum [64]

A similar application for crude fatty acids was patented by Lausberg *et al.* [84] to obtain fatty acids with improved odor, color and heat stability with a so-called precut column. The purpose of the precut column is to separate the low-boiling color bodies and odor substances from the fatty acid feed before it enters the main column. Both the precut column and the main column make use of rectifying and stripping sections, high vacuum (1-20 mbar for precut column, 1-50 mbar for main column) and temperatures between 180 and 280 °C. Structured packing like Sulzer Mellapack, Montz-Pak or Kuhni Rombopack were recommended and superheated steam stripping was applied to the latter column. [84] The precut column is similar to the pre-flashing tower in a crude oil distillation unit, but the purpose is not exactly the same. While the pre-flash tower in petroleum industry enhances the unit operations, capacity and energy-efficiency of the unit, the precut column aims for the better separation of impurities. It enables better separation of the already existing low boiling species as well as the ones that are generated during the distillation due to the thermal degradation. [84, 64]

4.2 Multistage distillation and applications

Flash distillation includes only one separation stage which means that by dividing the feed to two streams, the yield of pure components is poor. By connecting several stages, the separation efficiency can be enhanced. In practice, the series of separation stages is realized as a distillation tower or column [81]. Figure 4.4 by Kleiber [57] demonstrates the typical distillation arrangement and terms. The feed that is to be fractionated by distillation, is continuously pumped to the column. The section above the feed location is called the rectifying section and the part below is the stripping section. At the bottom of the column, a reboiler generates vapor that works as a heat input for the column. The vapor rises through the internals, trays or packings that enable a good contact and mass transfer between vapor and liquid phase. The overhead stream is condensed and part of it is led back to the column as reflux. The reflux stream forms an essential countercurrent flow together with the rising vapor. [57]

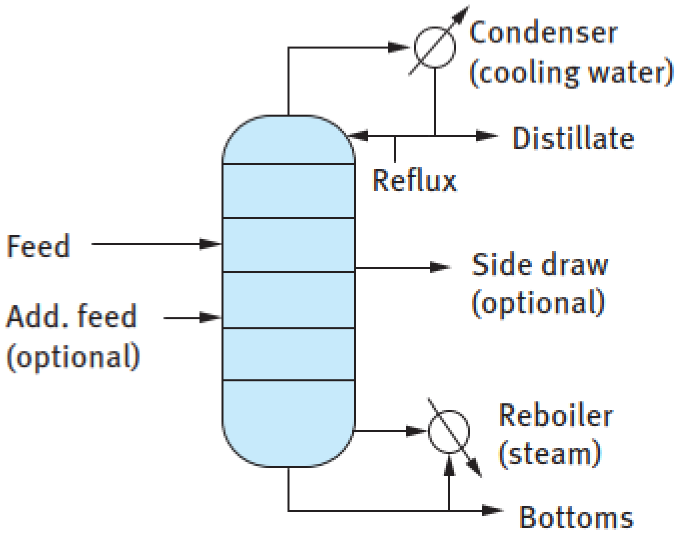

Figure 4.4 Distillation column and the most important terms [57]

Luyben [85] describes the McCabe-Thiele method which is a graphical approach showing the effects of vapor-liquid equilibrium (VLE), reflux ratio and number of trays. It is limited to binary systems, but the parameter effects can be extended to multicomponent systems. Approximate methods for multicomponent distillation have also been developed for obtaining estimates of the column size (number of trays) and the energy requirements (reflux ratios and the corresponding vapor boilup and reboiler heat input). Such methods include Fenske equation for minimum number of stages and Underwood equations for minimum reflux ratio. Without going into details of these methods, some general relationships and assumptions in distillation can be stated:

- Easy separations require fewer trays but if higher product purity is desired, more trays are needed.

- Increased purity does not have a remarkable effect on the required reflux ratio.
- A higher reflux ratio increases energy input (reboiler heat input) requirements.
- The increased liquid-to-vapor ratio in some section of a column benefits the separation of that section.
- Lower relative volatilities make separation more difficult and require more trays or higher reflux rations. [85]

Kleiber [57] states that a real distillation tray doesn't accurately represent a theoretical separation stage and that efficiencies, which usually range around 2/3, should be introduced (e.g. 30 trays represent 20 equilibrium stages). With the concept of theoretical stages, the necessary number of separation stages and the reflux ratio can be determined by solving the so-called MESH equations (material balance, phase equilibrium, summation condition, heat balance). For a column with N stages and n components, the equations are:

- Material balance for each component on each stage: $n * N$ equations.
- Phase equilibrium conditions for each component on each stage: $n * N$ equations.
- Summation conditions, $\sum x_i = 1 \sum y_i = 1$, on each stage: $2 * N$ equations.
- Heat balance on each stage: N equations.

All $N * (2n + 3)$ equations have to be solved. Modern process simulators offer stable and well-established algorithms for obtaining a solution. [57]

4.2.1 Column internals

The distillation tower internals consist of either trays or packings (or both), both having their strengths and weaknesses. Packed internals can be further divided into random and structured packings. Kleiber [57] and Nag [64] presented guidelines for choosing the right internals depending on the process parameters and they have been briefly combined and listed below:

1. Pressure drop: The pressure drop of the packed columns is significantly lower than tray columns. Packings are more or less obligatory for high vacuum distillation systems because of smaller column sizes.
2. Side-streams: Side-streams are easily provided for tray columns. Packed columns require chimney trays for side withdrawal.
3. Fouling: Structured packings are the most sensitive against fouling while random packings do not cope well either. Trays, especially sieve trays with

large holes can cope better with fouling and handle even a certain amount of solids.

4. Foaming: Packings, especially random packings, can cope with limited foaming whereas trays are not suitable for foaming systems.
5. Corrosion: Packings could be cheaper, because they can be manufactured of plastic or ceramic to avoid corrosion. Trays would be made of expensive metals in order to resist corrosion.
6. Diameter: For small columns (d < 800 mm), packed columns are more suitable. The installation of trays would be difficult and packing replacing might be cheaper if it becomes fouled.
7. Loads and reliability: Tray columns cope with variating liquid loads, but are relatively sensitive towards variation of the vapor load. Random packings don't function well with low liquid loads while the structured packings have difficulties with higher liquid loads. Liquid distribution of the packed columns is vital and the choice of distribution system plays a big role with packed columns. The likelihood of improper liquid distribution with packings makes trays a more reliable choice on this matter.
8. Aqueous systems: The high surface tension while handling aqueous systems or lighter hydrocarbons could prove to be problematic with some packings.
9. Residence time: The residence time is lower in packed columns partly because of the smaller size and they are advantageous to avoid undesired reactions. The residence time of the trays is well defined and should be used in reactive distillation.

4.2.2 Vacuum and overhead system

Vacuum systems in vegetable oil deodorizers and fossil crude oil vacuum distillation columns are often generated with ejectors [86-88, 64]. Ejector systems may be configured in a number of different ways depending on the distilled material and refinery operations. A single vacuum train consists of one set of ejectors and condensers allowing the lowest initial investment. The flexibility in utility (often steam) control and managing different crudes and unit operations can be increased with parallel ejectors on each stage of the vacuum train [87]. Habibullah *et al.* [86] state that steam ejectors are usually specified as three-stage units for most crude oil vacuum distillation units. Figure 4.5 represents such system for the wet vacuum crude distillation column. The wet system includes a pre-condenser, which is not a necessity for a dry vacuum column that operates without stripping steam. [86] Gupta [88] reports that the most modern vacuum systems in deodorizer units have four stages.

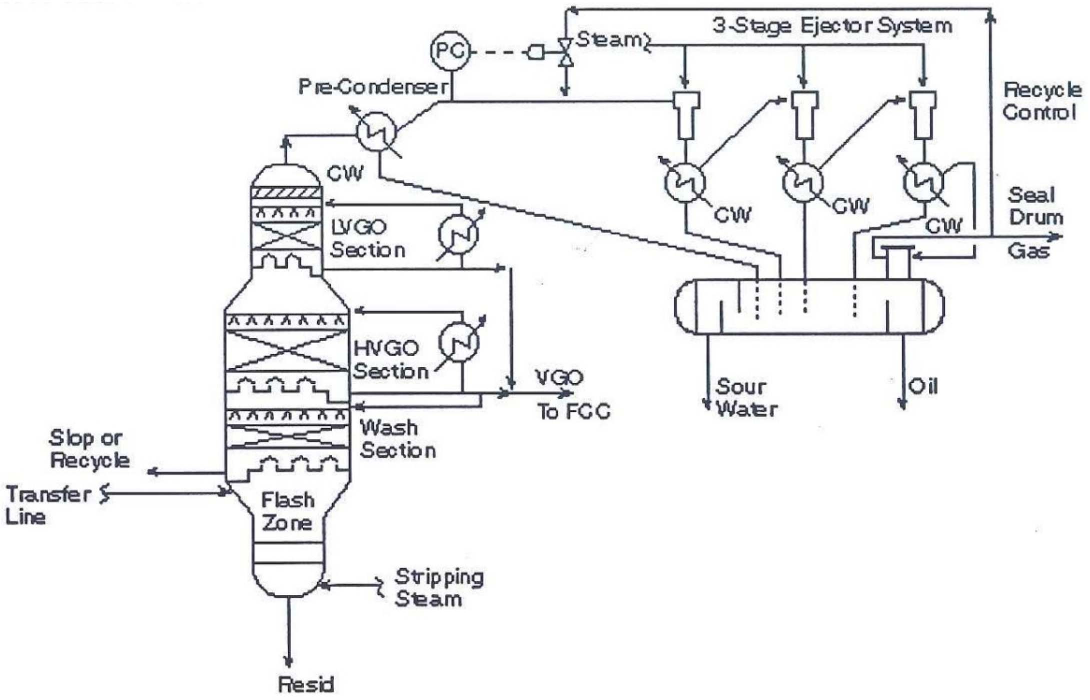

Figure 4.5 A three-stage ejector system for the wet crude oil vacuum column [86]

An ejector and its main parts are illustrated in Figure 4.6. The ejector's operating principle is to convert pressure energy of the motive fluid, which often tends to be steam, into velocity. The motive fluid is fed through a converging and diverging nozzle where adiabatic expansion occurs. As a result, the motive fluid achieves supersonic velocity off the nozzle and expands to a pressure lower than the system's suction load pressure. This creates a low-pressure zone for pulling the system's suction load into ejector. The motive fluid and the suction gas load are mixed and the mixture enters a diffuser with supersonic velocity. The velocity decreases in the inlet section of the diffuser and the pressure is increased. In the throat section, a normal shock wave is established and a dramatic boost in pressure and loss of velocity occurs. The pressure keeps increasing and the velocity keeps dropping in the diverging section and the mixture is led to a safe place, e.g. a container. [87]

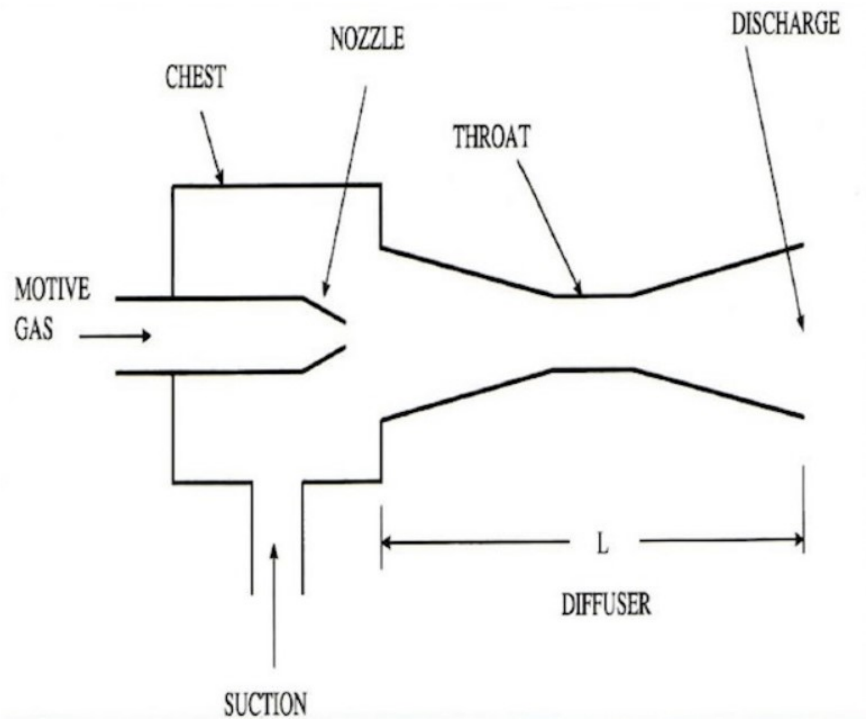

Figure 4.6 An ejector and its main parts [89]

Ejectors are the simplest equipment to produce vacuum since they have no moving parts. Their problem is, however, the high energy usage (steam consumption). For example, liquid-ring vacuum pumps or dry vacuum pumps have been used to replace the third ejector stage in order to cut down the energy penalty. Liquid ring pumps cannot, however, achieve the very low pressures required by modern ejectors on a reliable basis. [88, 86] The latest trend in vacuum ejector design for deodorizers is the freeze condensing unit which reduces the size and steam consumption of the ejectors [86].

4.3 Distillation of fatty acid mixtures

Purification of fatty acids by distillation has also been practiced for over a hundred years and it is used to remove both the low and high boiling impurities as well as odor substances [90]. It has also been used for fractionating the fatty acid mixtures to different products according to the carbon-chain lengths. The first such fractionating unit was installed in 1933 by Armour and Company which included the main fractionating tower, two smaller side stripping towers, conventional air ejectors and boosters, condensers, coolers and a direct-fired fatty acid heater. The fatty acids are sensitive towards heat which promotes the usage of as low temperature as practically and economically possible while maintaining the shortest residence time of the fatty acid in the distillation column. [90] The modern fatty acid distillation apparatus presented by Lausberg *et al.* [84] works under high vacuum (< 50 mbar) as well as most of the other distillation concepts involved in fatty acid purification in order to avoid the production losses [21]. Figure 4.7 shows a fatty acid fractionation concept where low-boiling components are first removed in the fractionation column and the remaining fatty acids are separated in the distillation further according to their chain length [91].

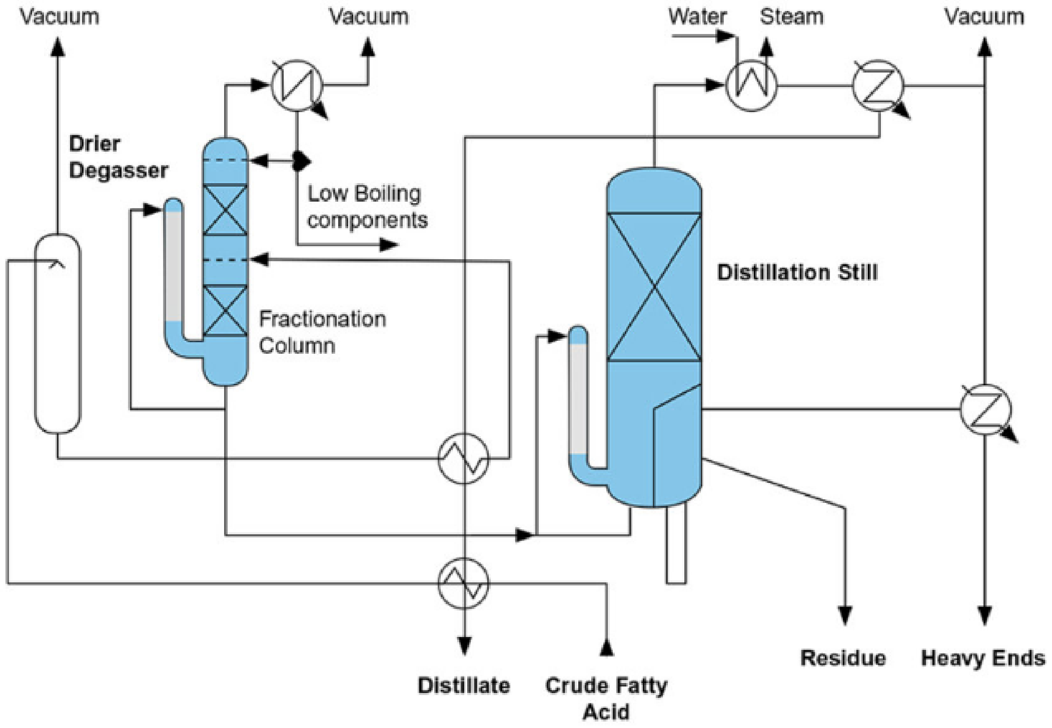

Figure 4.7 A two-stage fatty acid fractionation design [91]

4.4 Deodorization

Deodorization is a well-known concept in the vegetable oil refining and usually the last step in the refining sequence. It is a steam distillation process which is carried out at high temperature (200 – 260 °C) and low pressure (2.5 – 9.2 mbar).The purpose of deodorization concept is to remove trace components, which give the oil its characteristic, unpleasant taste and odor. Deodorization also affects in the reduction of free fatty acids and decolorization of some pigments, natural tocopherol, tocotrienol antioxidants and other unsaponifiable material such as sterols, hydrocarbons and alcohols. Deodorization also removes almost all the pesticide residues, polycyclic aromatic hydrocarbons (PAHs) (those with four or less benzene rings in their structure), final traces of any extraction solvents and volatile sulfur compounds. [21]

The whole deodorization process involves various steps. The refined and bleached oil is deaerated at a temperature of 85-90 °C under the same vacuum occupying the deodorizer. The oil is then preheated to a temperature of 249-254 °C under the same vacuum prior to deodorization. The steam distillation happens at low pressure and saturated steam is injected at the bottom of the oil bed in the deodorizer. The temperature should be maintained below 260 °C because several vegetable oils start to polymerize at higher temperatures. The deodorized product is cooled down to 143 °C and 50% citric acid is added to reduce any remaining trace metals. The oil is further cooled to 127 °C, pumped out of the deodorizer and eventually cooled to its oil-specific storage temperature. A schematic view of fully continuous deodorizer is presented in Figure 4.8. [88]

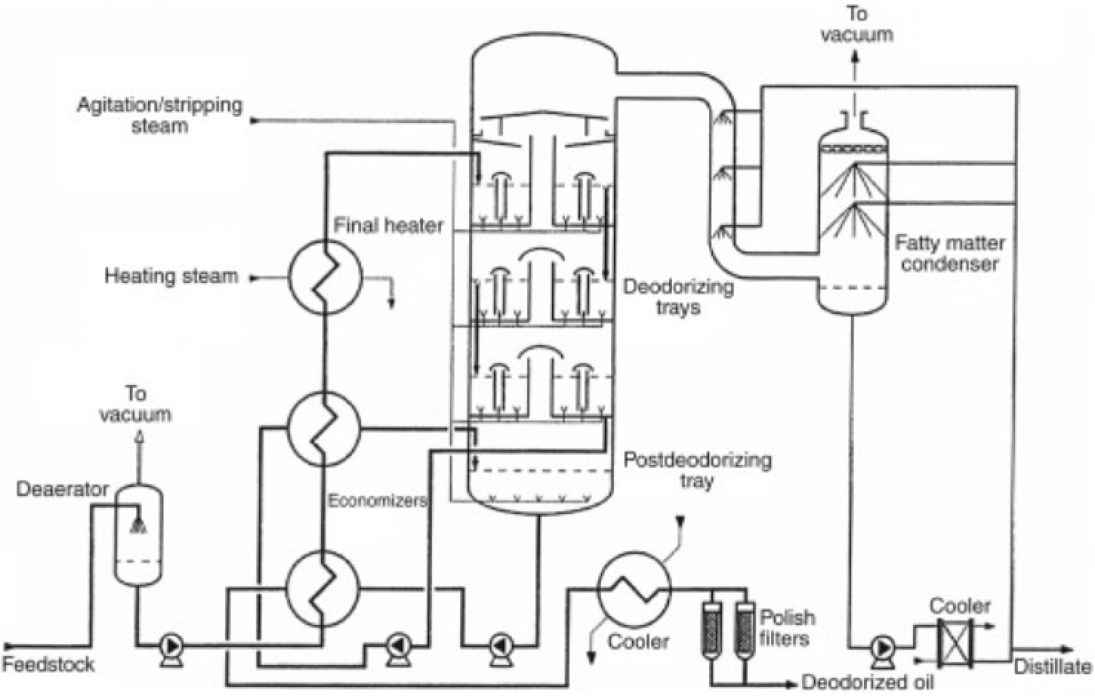

Figure 4.8 A fully continuous deodorizer design [88]

The deodorization process as a pre-processing method of the impurities removal could still prove to be problematic. Both Gupta [88] and Erickson [92] have discussed the strict restrictions of the incoming feedstock. According to the authors, the amount of impurities to be handled is limited, without exception, to the values presented in Table 4.1.

Table 4.1 Feedstock quality requirements prior to deodorization [88]

Substance	Amount
Phosphorus	< 1 ppm
Chlorophyll	< 30 ppb (parts per billion)
Iron	< 0.2 ppm
Calcium	< 0.2 ppm
Magnesium	< 0.2 ppm
Nickel (From hydrogenation Ni-catalyst)	trace (< 0.5 ppm)

The values in Table 4.1 however refer to the last purification step of manufacturing edible oils, where the desired level of product impurities is extremely low. For example, phosphorus level cannot be reduced by deodorization and thus needs to be initially low. Some hydrolysis also takes place during the steam stripping and the produced FFA is immediately removed. However, phosphorus, which is a natural emulsifier present in the oil at high level, drives some additional hydrolysis. This results in the higher undesirable FFA amounts in the deodorized oils. To avoid this, either the residence time, temperature or both in the deodorizer should be raised. [88]

4.5 Short-path distillation

Short-path distillation (SPD) has been around for a long time and has been under development even before the Second World War [93]. The modern, commercial SPD units are either of falling film type or centrifugal type. The falling film is a more common type, where the thin film is generated by devices such as rollers, wipers, fixed clearance blades, or pitched blades rotating inside the column to spread out the film. The second method uses a rotating disk that spreads a film through the use of centrifugal force on a heated disc. [94] The centrifugal type will not be further discussed and with all further references to an SPD unit, the falling film type is meant.

The modern SPD unit relies on short residence time of the product in the evaporator (< 10 seconds), very low operating pressure (< 0.01 mbar) and short distance (10-50 mm) between the internal evaporator and condenser. The short distance between heating and cooling allows for minimal pressure drop, which enables the deep vacuum conditions. SPD units are typically jacketed vessels as illustrated in Figure 4.9. The feed is equally led into the heated surfaces with the help of an agitator and several components are evaporated. The evaporated components travel a short distance and almost immediately condense on the cold surface. The condensate and the distillate are collected from the bottom of the apparatus. [95, 94]

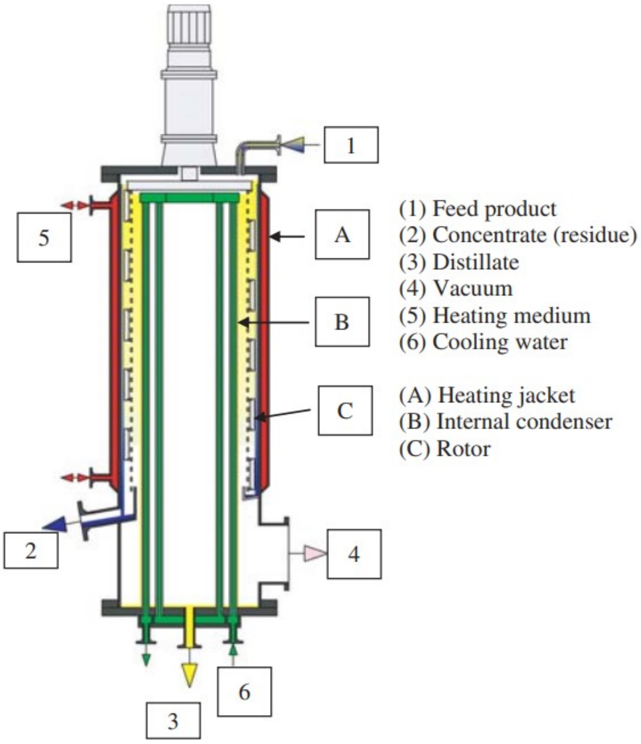

Figure 4.9 Schematic view of a falling film type short-path evaporator [95]

Both De Greyt (2013) [95] and Xu *et al.* [96] stated in 2013 and 2002 respectively that the SPD technology has not yet established in the vegetable oil and fat industry though it has been implemented in some specific processes. Such processes include production of high-purity monoacylglycerols, concentration of omega-3 fatty acids, downstream processing of deodorizer distillates, production of red palm oil (rich in carotenoids) and contaminant removal from fish oil. The problems limiting SPD's broad implementation consist of high investment and operating costs. [95, 96] It has also been emphasized that the residence time is too short for the production of stable, odorless and bland distillate [95]. Alasti *et al.* [94] also reported that the SPD operates at relatively low distillation rates of 100-200 kg/h per m^2 of evaporator surface area.

4.6 Cost estimation of distillation equipment

Costs are divided into capital investment (CAPEX) and operating costs (OPEX). OPEX can be further divided into fixed costs (e.g. operating labor) and variable costs, which are proportional to the production output (e.g. raw materials and utilities). [57]

The foundation of fixed capital investment estimate is the equipment cost data. By application of factors or percentages to the equipment cost data, the fixed capital investment is developed. The equipment cost data is often presented as cost-capacity plots that indicate a straight-line relationship on a log-log plot. An example of such plot for atmospheric sieve tray column from the year 1998 is presented in Figure 4.10. Some of these plots are quite old and one bids from vendors should be requested in order to obtain current cost data. A disadvantage of using vendor quotations is, however, risking proprietary information. [97] A distillation unit working in vacuum requires, in addition to the actual fractionation column, also side-stripping columns, several heat exchangers (preheating, condensers, reboilers), pumps, vacuum ejectors or vacuum pumps and overhead vessels. In addition to large apparatus, piping, valves and instrumentation is also needed.

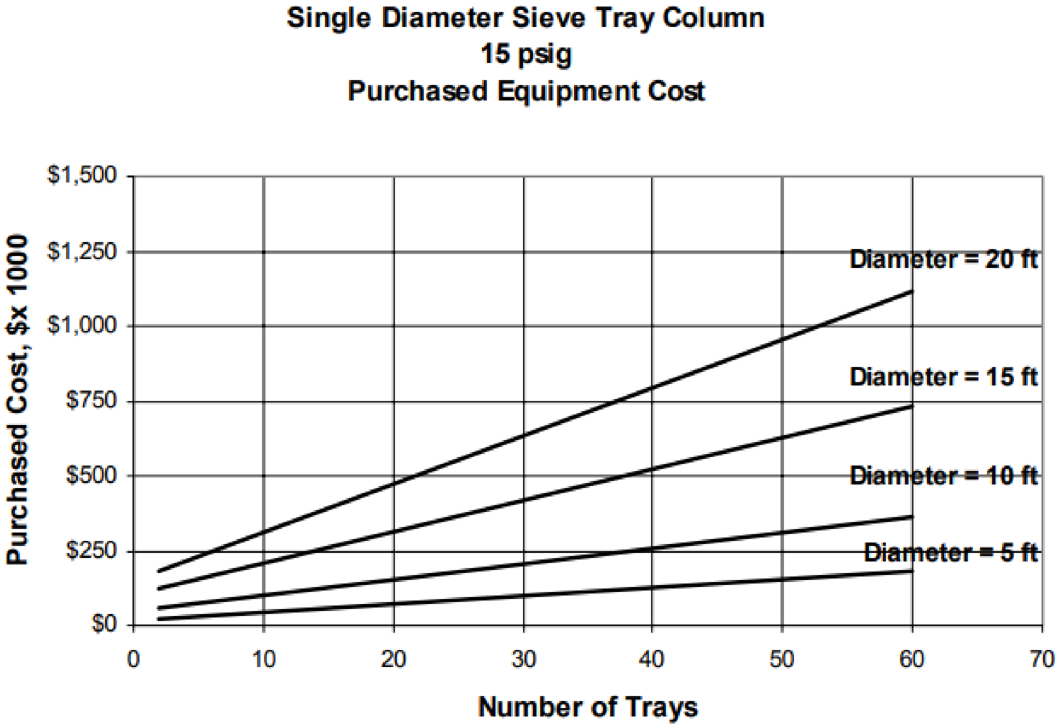

Figure 4.10 Cost-capacity plot for an A515 carbon-steel column [98]

For preliminary cost estimation, Hand factors, that are refined from Lang factors, can be applied. These factors are multiplied by the estimated equipment prices to find out the final, installed cost of equipment. Other, more detailed factors, such as Wroth factors, have also been developed to serve the same purpose. One thing to note is that Lang and Hand factors do not include delivery charges. Hand factors are presented in Table 4.2. [97]

Table 4.2 Hand factors for equipment [97]

Equipment type	Factor
Fractionating columns	4.0
Pressure vessels	4.0
Heat exchangers	3.5
Fired heaters	2.0
Pumps	4.0
Compressors	2.5
Instruments	4.0
Miscellaneous	2.5

The operating expenses (OPEX) consist of the costs of utilities, raw materials, operating labor, supervision, maintenance, environmental control etc. [97]. Utilities for distillation systems include steam (vacuum ejectors and column reboilers, possibly stripping steam, steam tracing, steam injection to feed or/and heating media to some heat exchangers), electricity (e.g. pumps, electric tracing), cooling water (e.g. condensation system), fuel/ fuel gas (e.g. steam generation), compressed air/instrument air (e.g. control valve with pneumatic actuator). Utilities might also include hot oil systems or refrigeration.

Modern processing plants strive for self-sufficiency. The preheating trains are often integrated with the product streams and steam generation can be done in furnaces that can possibly be heated with produced side-streams. Electricity is, however, needed for pumps and possibly heat generation. Steam is also often bought from outside the processing plant to some extent.

5 Distillation in Aspen Plus

In this chapter, different distillation models of Aspen Plus are introduced and methods for gaining information about the system are discussed. Suitable property methods for distillation and triglycerides are also addressed. Aspen Plus can handle steady-state and dynamic simulations. If dynamic simulations are performed, all the components around distillation column should be defined including control valves and pumps. [85] William Luyben's [85] "Distillation Design and Control Using Aspen Simulation" serves as an excellent guide to simulation of distillation in Aspen Plus and will be mostly referred in this chapter.

Aspen Plus contains a wide variety of property methods suitable for different unit operations. It is important to select an appropriate physical property method that will describe the phase equilibrium in the most accurate possible way. The recommended models for the low pressure applications like vacuum and atmospheric crude towers are Chao-Seader, Braun K-10 and Grayson-Streed. These models are also suitable for petroleum applications [99]. Suthar *et al.* [100] compared the different property methods used in FAME biodiesel studies, which deal closely with triglycerides, FFA and alcohols (methanol & ethanol). Most of the studies conducted in Aspen Plus used NRTL, UNIQUAC and UNIFAC packages in order to predict the binary interaction parameters between the compounds and the vapor-liquid equilibrium (VLE) conditions. [100] UNIFAC has become very popular in the past several decades. It uses functional groups of molecules for the prediction of vapor-liquid equilibria. This is convenient as the experimental data is often not available for a wide variety of different compounds. [101] Luyben notes that different physical property packages can be selected for different unit operations in a flowsheet and the best one should be picked for each separate case [85].

There are many different column types to choose from. The shortcut distillation designs include DSTWU, Distl and SCFrac models. The rigorous models consist of RadFrac, Extract, MultiFrac and PetroFrac. The shortcut methods assume constant relative volatiles and constant molal overflow which means that these methods should not be used for systems that deviate significantly from the mentioned assumptions. The rigorous models have a larger variety of parameters that can be defined in order to get accurate models. RadFrac handles all types of multistage vapor-liquid fractionation operations. It is suitable for two- and three-phase systems, narrow and wide-boiling systems and systems with strong liquid phase nonideality. MultiFrac can work with several number of columns linked with each other. It can be used to model large systems like Petlyuk towers, air separation column systems, absorber/stripper combination, ethylene plants, etc. PetroFrac is designed for complex vapor-liquid fractionation operations in the petroleum refining industry. These operations include pre-flash towers, atmospheric crude unit, vacuum unit, catalytic cracker main fractionator, delayed coker main fractionator and vacuum lube fractionator. [99]

A step-by-step guide about setting up a steady-state simulation with the RadFrac model, as well as several other far more complicated cases, are provided by Luyben [85]. He illustrates how to build a flowsheet, define streams and chemical components, choose the property method, specify parameters of equipment, run the simulations and analyze results. The economic optimization is also gone through, where the basic idea is to find out the optimum number of stages. Some handy methods for gaining information about the distillation system are presented below:

- The optimal feed tray placement can be found iteratively by changing the stage of incoming feed. Then the reboiler heat input, condenser heat removal and reflux ratio can be analyzed in each iteration and the most energy-efficient alternative is chosen.
- The minimum reflux ratio can be defined by increasing the amount of distillation stages until the reflux ratio does not remarkable decrease.
- The minimum number of trays can be specified by decreasing the amount of distillation stages until the reflux ratio becomes notably large. [85]

The height of a distillation column can easily be calculated when the number of stages and the typical tray spacing of 0.61 m is known. Aspen defines reflux drum and reboiler as stages that are not included in the equation $(N_T - 2)$. In addition to tray spacing, a factor of 1.2 is added which takes into account top and bottom spacing. The height equation then becomes:

$$L = 1{,}2(0{,}61)(N_T - 2) \qquad (1)$$

where L is the height of column and N_T is the number of stages including reboiler and reflux drum. The column diameter is determined by the maximum vapor velocity. If the velocity is exceeded, flooding occurs. The diameter is calculated by Aspen Plus and it can be checked with the following equation:

$$F\ factor = V_{max}\sqrt{\rho v}. \qquad (2)$$

Here, the “F factor” should be equal to 1 (in English Engineering units), V_{max} is the maximum vapor velocity in ft/s and ρv is the vapor density in lb/ft^3. [85]

Simulation of a distillation column is an iterative procedure. If the simulation does not converge at all, the convergence history should be studied. Common errors can indicate that either the liquid or vapor phase are missing from a specific stage of distillation column. This means that specifications should be changed so that the amount of missing component on that stage is increased. If the error message states that the specified bottom or distillate flow is larger than the feed, the algorithm has no chance to converge. [57]

One thing to note is that Aspen Plus does not have vacuum pump nor ejector models. If an accurate vacuum generation system is desired to be created, these models have to be manually built from the existing blocks. A Korean patent describes how an ejector type refrigeration and purification system is built in Aspen Plus and it is presented in Figure 5.1. Compressors work as the suction nozzles, the mixing block is the chamber, decompressor is the convergent section of the diffuser and a compressor is the divergent section. [102]

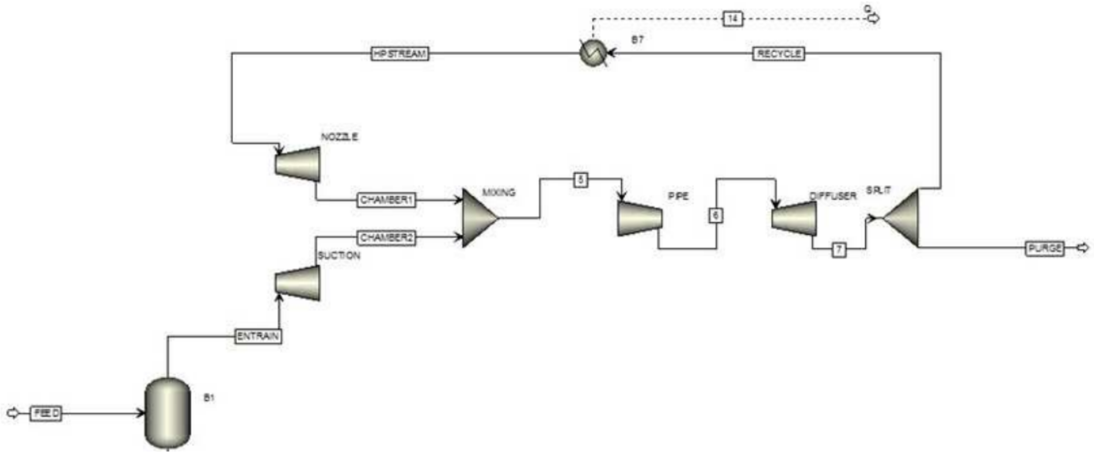

Figure 5.1 An ejector modelled from existing blocks in Aspen Plus [102]

APPLIED PART

Purpose of the applied part of this Master's thesis is to investigate separation of free fatty acids from triglycerides in a fat feedstock by distillation in the Aspen Plus V10 simulation environment. The two most promising distillation concept are the side-stream distillation column concept and the pre-flash and simple distillation column concept. Results are gathered and the main variables influencing the concepts and their operability are analyzed and discussed. The turndown range of the developed side-stream column concept is established and studied with respect to free fatty acid content of the fat feedstock. Operational costs of the concepts are also calculated. Comparison between the two concepts is performed.

6 Separation of free fatty acids from fat feedstock

This chapter describes the feed and individual components used as the base case in simulations. The separation process between the free fatty acids and glyceride components is discussed and analyzed with the help of VLE-diagrams and Aspen's shortcut distillation method.

6.1 Feed characterization

A feed containing a high weight percent of FFA (65%) was chosen as a base case for simulations in order to model a decomposed waste fat or oil. The fatty acid profile of FFA was constructed according to Hayaan, *et al.* [13]. The glyceride fraction of the simulation feed included tri-, di- and monoglycerides. The amount of di- and monoglycerides, in the base case, was decided with the help of Chow's *et al.* [103] research. It states that neutral lipids in oil droplets consist of 83% triglycerides, 8% diglycerides and 0.5% monoglycerides. The triglycerides were scaled to 24.3% due to allow for the selected high feed FFA content, but di- and monoglycerides were kept the same, again, to model highly decomposed oil. Glycerides in the simulation were modelled as purely palmitic or oleic (P, PP, PPP, O, OO, OOO). Moisture content was chosen to be as high as 2.2% based on data presented by Suwanno et al. [12].

Various impurities including organochlorides and VOCs were added to the feed in order to evaluate their separation in the process, as they may have a severe impact on the material choices of the distillation apparatus due to corrosion. Three types of 3-MCPD organochlorides, according to Seefelder *et al.* [104], were added to feed. The lightest component, 3-MCPD, is available in the Aspen Plus V10 databank but the two heavier components, 3-MCPD mono- and diesters were added as user defined components. 20 ppm of each organochloride were added to the base feed. The VOC components were selected based on results presented by Wu *et al.* [50], as nine components from their study were added to feed.

A full feed composition is presented in Table 6.1.

Table 6.1 Feed composition of the base case

Substance	mass-%	Substance	mass-%
Lipids	97.8	Water	2.2
Glycerides	32.8	**Substance**	**mass-ppm**
PPP	10.4	impurities	442.9
OOO	13.8		
PP	3.4	VOCs	382.9
OO	4.6	ethanal	3.9
P	0.2	propanal	11.2
O	0.3	pentanal	38.9
		hexanal	162.8
FFA	65.0	pentanol	68.6
C6:0	0.01	Propanoic acid	3.6
C8:0	0.07	Butanoic acid	0.8
C10:0	0.06	Pentanoic acid	7.7
C12:0	0.9	Hexanoic acid	85.4
C14:0	1.0		
C16:0	28.0	Organochlorides	60.0
C18:0	2.8	3-MCPD	20.0
C18:1	25.8	3-MCPDME	20.0
C18:2	6.4	3-MCPDDE	20.0

6.2 Separation process analysis

In order to separate a pure FFA fraction from the glyceride fraction in the distillation process, the lighter components, such as water and VOCs, have to be removed. The distillation process was initially studied with the help of VLE-diagrams as many authors suggest [105, 85, 57]. The separation of FFA and the heavier glycerides (di,-tri-) is essentially quite easy due to large difference between the boiling points. The Txy diagram, presented in Figure 6.1, only shows minor non-ideal behavior between the lightest diglyceride (PP) and the heaviest free fatty acid (C18:0) at 1 bar.

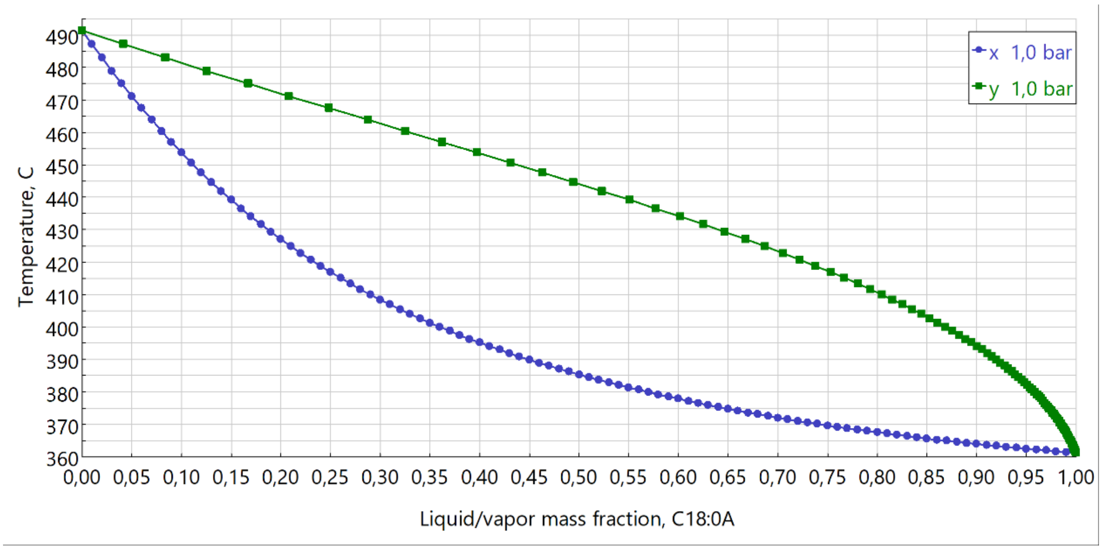

Figure 6.1 Txy diagram of dipalmitin and stearic acid at 1 bar

The feed includes a small amount of monoglycerides that produce a quite different binary Txy diagram together with C18:0 at 1 bar. Txy diagram between monopalmitin and stearic acid is presented in Figure 6.2. The substances form a homogenous azeotrope at the “pinch point” where the saturated liquid and vapor curves meet [105]. In practice, this means that it is not possible to produce both high purity monopalmitin and stearic acid in a single distillation column [105].

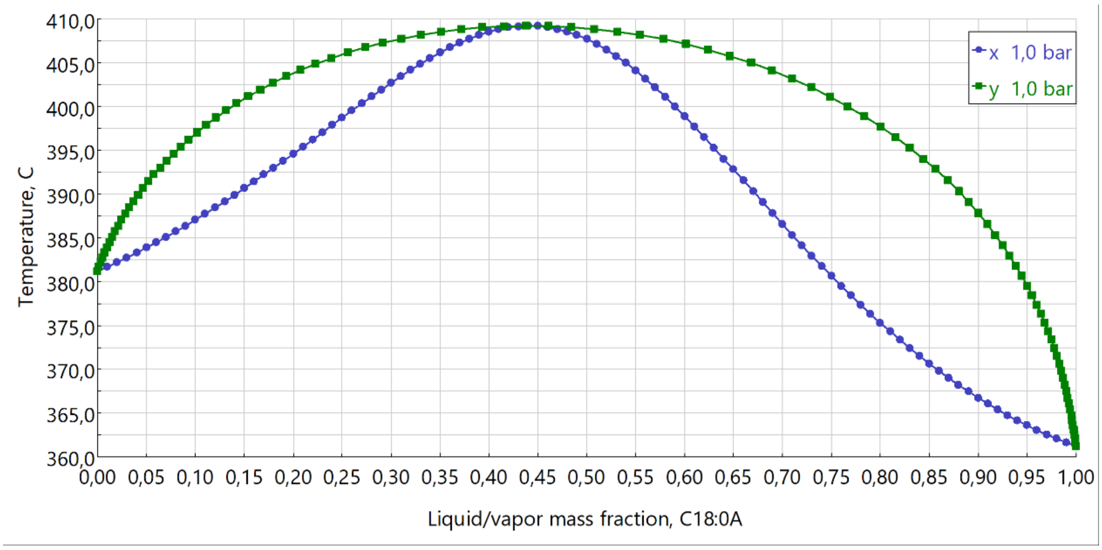

Figure 6.2 Txy diagram of monopalmitin and stearic acid at 1 bar

One other thing to notice from the VLE diagrams is that the glycerides and free fatty acids have high boiling points. This becomes problematic as lipids start to thermally decompose at high temperatures. For example, deodorizers work at the maximum temperature of 260 °C in order to avoid production losses [21, 88]. This is achieved by implementing a high vacuum with the help of ejector systems. The same Txy diagram between monopalmitin and stearic acid was also produced at 10 mbar. As seen from Figure 6.3, stearic acid's boiling point is now a bit above 222 °C which suggests that a vacuum column should be implemented as also stated in literature [21, 84].

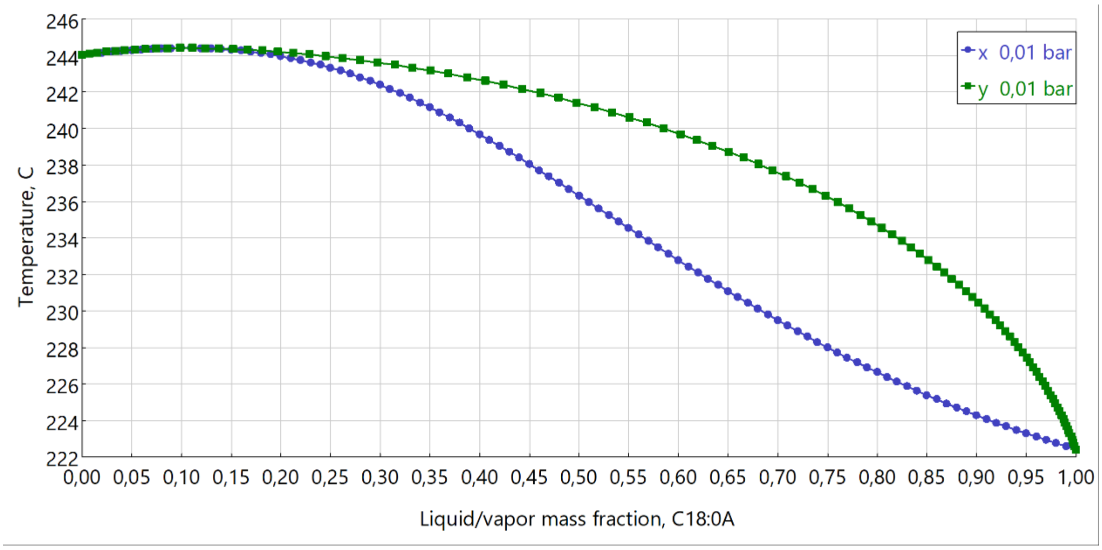

Figure 6.3 Txy diagram of monopalmitin and stearic acid at 10 mbar

It is necessary to notice that the lighter fraction, including water, VOCs, 3-MCPD and the lightest free fatty acids also has to be distilled from the FFA fraction. Water's boiling point at a deep vacuum (10 mbar) is, however, as low as 6.8 °C so it is not necessary to produce VLE-diagrams to analyze its separation.

The separation was further investigated with the help of Aspen's shortcut distillation model, DSTWU, before starting the simulation with a rigorous column model. DSTWU gives good predictions of the required separation stages and reflux ratio. It also gives information of the energy requirements, temperatures and even generates a table of reflux ratio vs number of theoretical stages, if the user so defines. This useful, initial data can be later implemented as starting values in order to help the Radfrac rigorous column model to converge. It should be noted that DSTWU is suitable only for ideal mixtures. For the non-ideal mixtures, the results might be considerably off [106].

The separation between monopalmitin and stearic acid was studied with the DSTWU model. The recovery percentage of light key component, stearic acid, was set to 95% and the recovery percentage of heavy key component, monopalmitin, was set to 1%.

Recovery percentages mean the amount of component in the distillate. Top pressure was set to 10 mbar and bottom pressure to 30 mbar. Partial condenser with all vapor distillate was selected and reflux ratio was set to 1.

With these input specifications, bottom temperature of the column rose to over 300 °C, which indicates a too ambitious stearic acid recovery percentage or an unnecessarily high monopalmitin recovery percentage. By changing the light key component to oleic acid (C18:1), setting its recovery rate to 70% and reducing the recovery rate of monopalmitin to 0.01%, the bottom temperature was successfully lowered to 260 °C, while keeping the FFA recovery around 80%. In order to satisfy these design conditions, a minimum of 4 theoretical stages are needed with a huge reflux ratio of 167.7. The calculated minimum reflux ratio was 0.14. The number of actual stages needed with the reflux ratio of 1 would be 5.6.

Several different concepts were initially considered and roughly tested in Aspen. The simplest concept included only a couple of flash drums where the idea was to first vaporize the water and then separate FFA and glycerides in the second flash. The separation of glycerides and FFA was, however, not as good as desired so the simplest concept was discarded. The two concepts that were investigated and further analyzed included multistage distillation columns.

7 Methods

The purpose of this chapter is to introduce the properties that were used in simulations and describe the definition process of the organic chloride components that are not included in the default databanks of Aspen Plus. The final side-stream column concept is introduced. A secondary concept including a pre-flash drum is also briefly reviewed.

7.1 Simulation properties and user-defined components

Dortmund modified UNIFAC was used as the base thermodynamic method in all simulations. Accuracy of the original UNIFAC is only guaranteed within a temperature range of 27 °C – 152 °C. The original UNIFAC model has also other weaknesses, such as poor reliability when compound sizes differ greatly from one another and limitation from low to moderate pressures. [107]

Dortmund modified UNIFAC includes temperature-dependent group interaction parameters that have improved results for the calculation of enthalpies of mixing. The inclusion of excess enthalpy data in the group interaction parameters fitting procedure has yielded improved predictions of these values. Comparisons between the different UNIFAC modifications shows that the Dortmund modification deviates less from experimental data. [107-109] 2018 revised and extended UNIFAC Dortmund group interaction parameters were implemented in all simulations.

Pure component properties for all the components used in the simulations, except for two organochlorides, were obtained from either an in-house databank or Aspen's default data banks. Two organochlorides, 3-MCPD monoester and 3-MCPD diester, were not available in in-house or Aspen databanks. Seefelder *et al.* [104] and Zelinková *et al.* [110] described the structures of these organochlorides and they are presented in Figure 7.1. It was decided, for simplicity's sake, that the alkyl group (R) was replaced with C16 in every case (C18 could have been also used). The structures of the components were drawn in Aspen and the SMILES (The Simplified molecular-input line-entry system) line notations were generated and extracted to ICAS ProPred. ProPred is a property estimation toolbox integrated within the ICAS software developed by CAPEC, DTU.

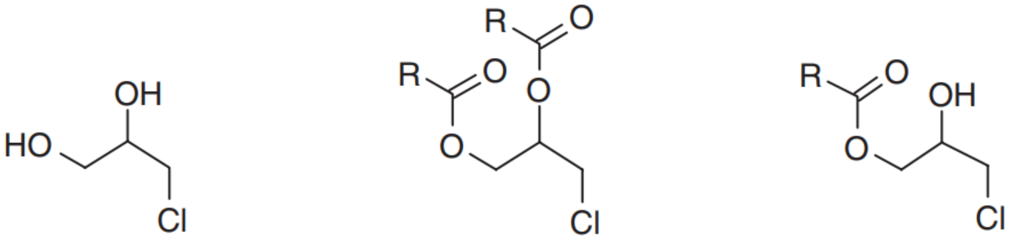

3-MCPD 3-MCPD diesters 1-monoesters of3-MCPD

Figure 7.1 Structures of free 3-MCPD, 3-MCPD monoester and 3-MCPD diester [104]

All the necessary pure component properties for distillation were estimated with the help of group contribution and atom connectivity index methods. Generated datasets of molar enthalpy of vaporization, liquid vapor pressure data and liquid molar volume were transferred to Aspen where regression of corresponding property model parameters was done. Molecular weight, normal boiling point, enthalpy of formation, standard free energy of formation for ideal gas, critical temperature, critical pressure, critical volume, critical compressibility factor and pitzer acentric factor were also extracted from ProPred to Aspen's pure component scalar parameters for the new components.

7.2 Side-stream column concept

The main objective of the side-stream distillation column concept was to achieve as good separation between FFA and glyceride fraction as possible, while keeping the column temperature preferably under 260 °C. The column was specifically designed and optimized for a 65% FFA base case feed. The secondary objective was to inspect if the same column geometry could be used for varying amounts of FFA content in the feed by considering the hydraulic operational range of specific internals.

The conceptual flow scheme is presented in Figure 7.2, where CW means cooling water and HO hot oil circulation. The feed is pre-heated with the side-stream (FFA fraction) to as high temperature as available. In the base case, feed is heated to 120 °C before leading it to the bottom of the distillation column where also a sufficient amount of steam is injected. The side-stream column concept was designed so that the overhead stream is as small as possible, containing mostly water. VOCs, 3-MCPD and the lightest free fatty acids were also destined to the overhead. The side-stream, consisting mostly of FFA, is drawn from the middle section of the column based on the volatilities of components as described in the section 6.2. The bottom stream contains mostly glycerides, which are the heaviest components. The side-stream and the bottom stream are cooled down to 60 °C prior to storage. The uncondensed gases were directed to a three-stage ejector system with barometric intercoolers. The small, condensed overhead stream fraction is safely discarded. It contains mostly light free fatty acids but also VOCs and unbound 3-MCPD. The ejector system was not modelled in Aspen Plus.

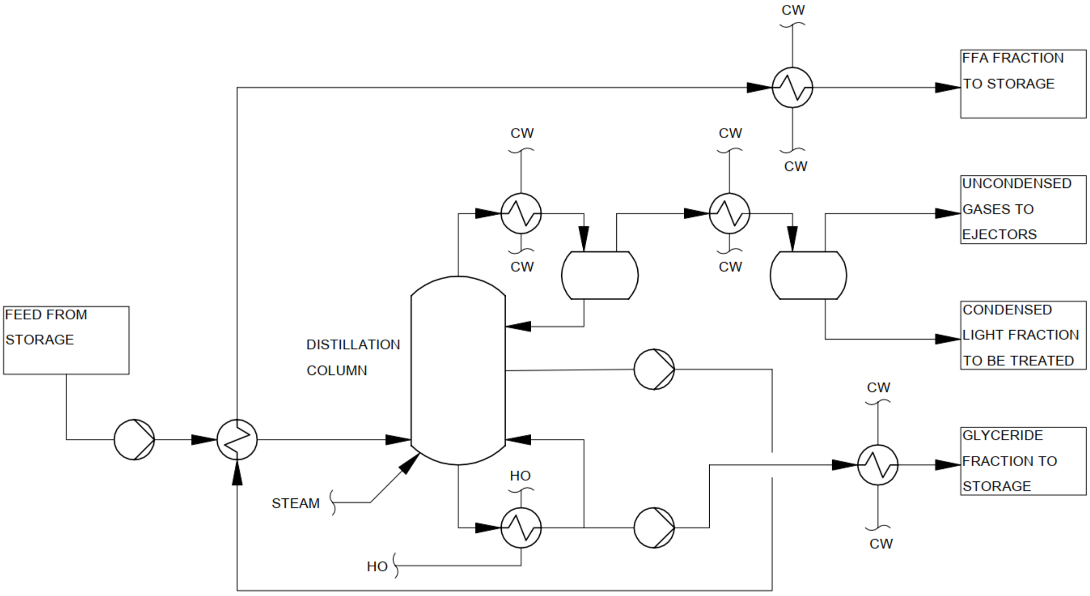

Figure 7.2 Side-stream distillation column concept flow scheme

The number of stages was selected as 8, based on the DSTWU's initial guesses and iterative testing. In Aspen Plus, the condenser and reboiler are considered as stages so the number of actual separation stages was 6. Stages are numbered from top to bottom with the condenser serving the function of the first stage. The feed enters the column from the bottom, under stage 8. As the nature of the column is such that the separation is quite easy, but the amount of liquid to be vaporized is large, it is necessary to direct the feed as close to the reboiler as possible. This reduces energy requirements of the reboiler as well as the bottom temperature. The side-stream, consisting of the free fatty acids, was drawn from stage 4. This way, the free fatty acids were effectively separated from the lighter and heavier components, yielding a pure FFA fraction. The lighter fraction, including water, VOCs, light FFA and unbound 3-MCPD was drawn from the top of the column. The heavier fraction, including glycerides, heavy FFA and bound 3-MCPD was drawn from the bottom of the column.

A partial-vapor condenser and kettle type reboiler were chosen for the column. Kister [111] states that kettle type reboilers are preferred in the applications where frequent cleaning is anticipated, particularly in vacuum columns. A hot oil circulation is needed for the reboiler as the required bottom temperature is quite high.

Top stage pressure was chosen to be 10 mbar. The deep vacuum was selected in order to keep the boiling points of substances low (< 260 °C), thus preventing the possible thermal decomposition [88]. Deodorization-type columns reportedly operate at even lower pressures [21]. Steam coupling (possibility to inject steam) was added below the bottom stage, where the feed comes in. The injection of steam lowers the bottom temperature, thus further preventing thermal decomposition of the lipids. Addition of steam coupling also increases flexibility of column operations. Fat feedstock quality, its water content and FFA content may vary but the possibility of adjusting the feed's volatility and viscosity by injecting a certain amount of steam, stabilizes the operations. Steam/water coupling should also be added to the pipeline leading to the distillation column. In the base case simulation, 400 kg of 15 bar steam at its saturation temperature was added to the bottom. Helmenstine [112] states that steam distillation is a common practice in petroleum refineries, isolation of essential oils and commercial separation of fatty acids. The goal of steam distillation is to lower the boiling points of the compounds and separate the components below their decomposition point [112].

Design parameters of the internals were slightly changed in order to obtain a more realistic picture of the performance. The maximum jet flood limit was set to 80% and the maximum downcomer backup was set to 60%. These changes were recommended in a training video titled "Getting Started with Column Analysis in Aspen Plus", published at the Aspen's Support Center as they now mimic typical vendor design limits in a better way. [113]

Efficiencies were introduced to every tray in the column because the real distillation column often have a Murphree efficiency of 0.6 – 0.7 [57]. Murphree efficiencies are often used in the equilibrium calculation to characterize the quality of a tray [57]. Murphree efficiency is defined as:

$$Eff_{i,j}^{M} = \frac{y_{i,j} - y_{i,j+1}}{K_{i,j}x_{i,j} - y_{i,j+1}} \qquad (3),$$

where $Eff_{i,j}^{M}$ is Murphree efficiency, y is vapor mole fraction, K is equilibrium K value, x is liquid mole fraction, i is component index and j is stage index [99]. Unfortunately, efficiencies may cause the liquid phase to be sub-cooled or super-heated in Aspen Plus if the efficiency is specified for all the components [99]. When the 0.7 Murphree efficiencies were implemented in the simulations, the top-stage froze. The freezing of the top-stage led to implementation of vaporization efficiencies where the named phenomena were not experienced. Efficiencies of 0.7 were defined to stages 2-7 (every separation stage). The main difference between Aspen's vaporization efficiency and Murphree efficiency is that the Murphree efficiency takes into account the adjacent stages while the vaporization efficiency is limited to the stage in question only. The vaporization efficiency is defined in the Aspen V10 user guide [99] as:

$$Eff_i^v = \frac{y_{i,j}}{K_{i,j} - x_{i,j}} \qquad (4).$$

Convergence of the distillation column was assisted in a couple of ways. The convergence method was changed from Standard to Petroleum/Wide-boiling at the column setup sheet. The used convergence algorithm was thus automatically changed to Sum-Rates. Maximum iterations were also changed from standard 25 to the Aspen's maximum of 200. An optional temperature estimate of 260 °C was also provided for the last stage in order to further ease the convergence. Used design specifications were liquid/vapor-mass ratio of the last separation stage and the overhead flow or the recovery of light components (Water + VOCs). Adjustable variables were reflux ratio and reboiler duty.

7.3 Pre-flash drum and simple column concept

In addition to the side-stream column concept, another type of distillation apparatus was designed and simulated with the base case values. The other concept included a pre-flash drum and a simple column without the side-stream draw-off. As the separation of light components and free fatty acids is considered as a rather easy process, it was investigated if it could be done effectively with only one stage (flash drum).

The pre-flash distillation concept flow scheme is presented in Figure 7.3. The feed was first pre-heated to 140 °C before leading it to the pre-flash drum. Pressure at the flash drum was kept at 10 mbar, the same as the main distillation column's overhead. Most of the water, VOCs, unbound 3-MCPD and the lightest free fatty acids are separated in the flash drum. The uncondensed gases are forwarded towards the ejector system which would be similar to the one described in the side-stream column concept. Here, a small condensed fraction of light free fatty acids is discarded as it contains VOCs and unbound 3-MCPD.

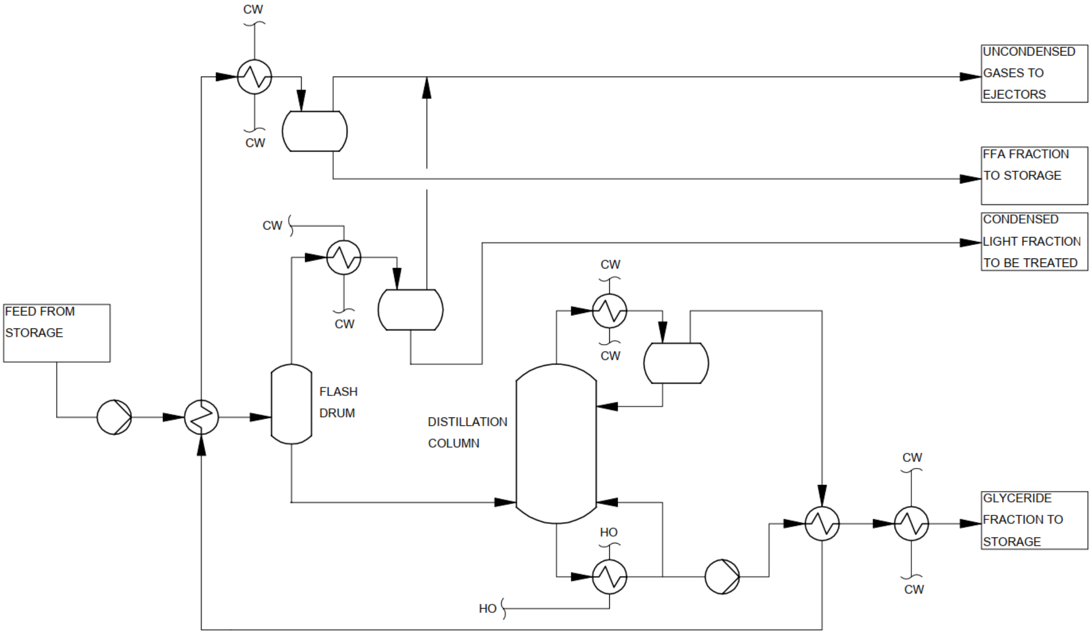

Figure 7.3 Pre-flash drum and simple distillation column flow scheme

The main separation between the FFA and glycerides was executed in a simple distillation column. The distillation column was similar to the bottom section of the side-stream column. It consisted of only five stages, including condenser, reboiler and three separation stages. One large difference to the side-stream concept is the absence of steam coupling. If a steam coupling would be present, another flash drum should be added downstream of the condenser. The overhead stream of the column is mostly FFA while the bottom stream consists of glycerides, the heaviest free fatty acids and bound organochlorides. The column internals were kept otherwise the same as in the side-stream column concept.

Compared to the side-stream distillation concept, an additional pre-heater was added to ensure that the overhead stream would be warm enough to heat the feed to 140 °C.

8 Results and Discussion

The purpose of this chapter is to present the results obtained from the Aspen Plus simulations of the two concepts. The main focus is on the side-stream column concept but many of the observed phenomena apply to the pre-flash concept. Different process variables and their influence on the distillation concept are discussed. A performance comparison between different column internals is carried out and the turndown ratio of the chosen column internals is discussed. Operational costs of the concepts are calculated. A comparison between the two presented concepts is also given.

8.1 Side-stream column concept results

8.1.1 Base case results

The complete side-stream column concept base case simulation results are presented in Table 8.1. As mentioned before, the main purpose of the column was to produce as good separation between the FFA and glyceride fractions as possible. The column was optimized to achieve 86.1% mass recovery of the free fatty acids to the side-stream in the base case feed. Slightly better yield could have been achieved, but this would have meant the bottom temperature rising over 260 °C or compromising process stability by operating the column near the hydraulic limits of the selected internals. Side-stream FFA purity of over 99.99% was achieved with a yield of 56% of feed in the side-stream. In the base case, the bottom flow was 41.2% of the feed and consisted mostly of glycerides 79.5% and the heaviest free fatty acids. Reboiler duty was near 4.8 MW and bottom temperature was about 258 °C. Due to high bottom temperature, a hot oil system for heating the boil-up stream was needed.

One clear drawback of the column is the high reflux ratio. Only 4.4% of the feed was directed to overhead in order to minimize maximize FFA separation to the side-stream. The overhead stream consisted mostly of water (86%) including a small amount of VOCs (0.9%) and 3-MCPD (0.04%), while the rest were light free fatty acids. The reflux ratio was 13.6. Condenser duty was about 2.5 MW and the reflux temperature was 103 °C. A large reflux ratio was necessary to satisfy column hydraulics by producing a sufficient liquid/vapor ratio inside the column. By raising the reflux ratio, the column diameter grows as more process fluid flows inside the column. Higher reflux ratio also affects the reboiler, as a larger heat duty is needed to vaporize more process fluid.

Table 8.1 Side-stream column base case simulation results

BASE CASE RESULTS	
FFA yield as side-stream (%)	86.2
Side-stream size (%)	56.0
Side-stream FFA purity (%)	99.991
Bottom stream size (%)	41.2
Bottom stream glyceride purity (%)	79.5
Specifications	
Liquid/vapor ratio at the bottom separation stage	0.27
Steam injection (kg)	400
Column results	
Condenser duty (MW)	2.6
Reflux ratio	13.6
Bottom temperature (°C)	258
Reboiler heat duty (MW)	4.8
Boilup ratio	2.1
Preheater duty (MW)	1.0
Feed temperature (°C)	120

8.1.2 Column internals and geometry

Selecting the most suitable column internals is critical to the overall performance of the column. The first question is often whether trays or packing is selected. In the base case simulation of the side-stream column concept, trays were selected. The two main reasons for this are the known weaknesses of packings: they are more sensitive to fouling and operation changes [57]. The fouling tendencies of the waste fat feedstock in the simulated cases are unknown and its composition may vary considerably. There were also concerns that waste feedstock might include solids, which packings do not tolerate [57]. Otherwise packings would be an ideal choice for this particular separation, as they produce a lower pressure drop reducing the bottom temperature [57]. According to Kleiber [57], they also make a design with a lower height possible at low pressures where systems exhibit larger separation factors.

Several different tray types were tested in Aspen, but Sulzer-Nutter BDP valve trays were superior in the end. The selected trays gave the smallest pressure drop and worked well with the low liquid/vapor ratios. Aspen Plus calculates tray pressure drop via the method described in Smith's 1963 book, "Design of Equilibrium Stage Processes" [99]. Trays were modified by increasing the number of valves per active area from 75 to 120 pcs/m2. This decreases pressure drop, but as a drawback, it lowers the tray's operation region by increasing the risk of weeping.

Challenges for designing the column internals were the large pressure variation in the column and the varying liquid-vapor distribution. With the selected internals, the bottom pressure of the column rose to almost 33 mbar according to the base case simulation, which is over three times more than the overhead pressure. The liquid mass flow was slightly higher than the vapor flow at the top stages (1-4), but below the massive side draw at stage 4, the amount of liquid on stages was considerably smaller compared to vapor (~ 1/4). As a result, the reflux rate has to be monitored carefully so that the bottom stages do not dry up.

As mentioned, the liquid loads below stage 4 are quite low. Kister [111] and Kleiber [57] recommend picket-fence weirs for trays with low liquid flow. Their job is to force back part of the liquid spray onto the tray and, thus, shorten the effective weir length. According to Kister [111], some authors recommend picketed weirs whenever the liquid load is under 0.5 - 1 gallons per minute per inch of weir (~ 4.47 – 8.94 cubic meters per hour per meter of weir) while the others would apply the weir modifications if the liquid load drops under 0.25 gpm per inch of weir (~2.24 m3/h/m). As the liquid loads for the last stages were smaller than 4.47 m3/h/m, picketed weirs were chosen and successfully deployed. The chosen picketing factor was 0.5, meaning that half of the weir surface is picketed. The picketed weirs allowed column operations at lower liquid loads giving the distillation process more flexibility. The drawback with picket-fence modification is a slight increase in pressure drop. All the other dimensions of trays were kept as Aspen Plus calculated them in interactive sizing mode for a 3.8 m diameter. The detailed tray dimensions are presented in Figure 8.1.

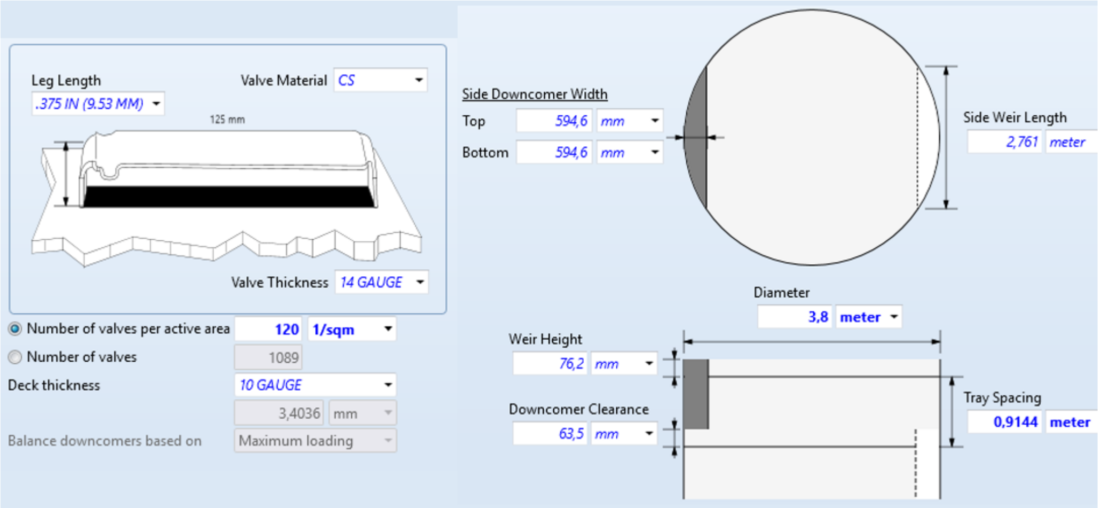

Leg Length: .375 IN (9.53 MM)
Valve Material: CS
Valve Thickness: 14 GAUGE
● Number of valves per active area: 120 1/sqm
○ Number of valves: 1089
Deck thickness: 10 GAUGE
3,4036 mm
Balance downcomers based on: Maximum loading
Side Downcomer Width
Top: 594,6 mm
Bottom: 594,6 mm
Side Weir Length: 2,761 meter
Diameter: 3,8 meter
Weir Height: 76,2 mm
Downcomer Clearance: 63,5 mm
Tray Spacing: 0,9144 meter

Figure 8.1 Valve tray dimensions used in base case simulation

On valve trays, holes are covered by movable valves. This gives the column operations flexibility and higher turndown as the valves open according to vapor load. Valve trays are the most common trays and approximately 20% more expensive than sieve trays. According to Kleiber, the pressure drop of valve trays is higher than of sieve trays. Weeping can usually be avoided, but the valve trays are sensitive to fouling. [57] The fouling problem most likely relates to sticking of the valves that is described by Kister [111]. Sticking occurs because of sludge buildup and corrosion while the valve is in contact with the tray floor. This reduces the open area of the tray and can initiate premature flooding. The moving legs of valves can also break, resulting in popping of the valves. [111] Fixed valve trays would solve both of these problems, as there are no moving parts. Fixed valve trays are basically sieve trays with covered holes [57].

Tray spacing was increased from Aspen’s default 24 inches (0.61 m) to 36 inches (0.91 m). The larger tray spacing is needed when frequent maintenance is expected due to fouling or corrosion. The diameter of the column is also large, which means that deep tray support beams are needed and they further restrict the crawling space (while maintaining the trays) and interfere with vapor movement across the tray, promoting a larger tray spacing. It is stated further that when operating in the spray regime (high vapor load compared to liquid load), larger tray spacing is recommended to avoid an excessive entrainment. Increasing tray spacing also reduces the column diameter, which may outweigh the manufacturing costs in designs with a low number of trays. [111] An increase in tray spacing, however, increases the pressure drop which is unfavorable in vacuum distillation of thermally sensitive components.

The designed column has a special geometry, as it has a large diameter but is rather short. The actual tray spacing, bottom sump height and column top section height should be discussed with a vendor. The bottom sump volume is calculated by multiplying the residence time with the volumetric flow rate of liquid leaving the sump (both boil-up stream and bottom stream) [111]. Then bottom sump height is further calculated by dividing the volume by the sump diameter. A sufficient residence time is needed in order to: provide sufficient settling time for separation, buffer the column from downstream or upstream upsets, give the operator time to react to process upsets and to disentrain vapor contained in the sump liquid [111]. Sump and top section calculations require further knowledge of the other process units and of the column control system. Therefore, they are not considered at the conceptual design level discussed in this thesis. In order to obtain a relatively realistic picture of the column height, top and bottom section heights are considered to be as long as the space between trays. Then the column height would be:

$$5 * 0.9144\ (tray\ spacing) + 0.9144\ (above\ top\ tray) + 0.9144\ (sump) = 6{,}4\ m.$$

A comparison of different column internals was performed. Six different tray types were tested. In addition, Sulzer Mellapack structured packing was also simulated as Lauberg *et al.* [84] recommend its usage in fatty acid distillation. Montz-Pak and Kuhni Rombopack were also suggested, but they were not available in Aspen Plus V10 [84]. The internals were optimized for base case feed so that the FFA yield as side-stream was 80% of the feed’s FFA with the exception of Sulzer-Nutter BDP valve trays where the FFA yield was 86%. Results are presented in Figure 8.2.

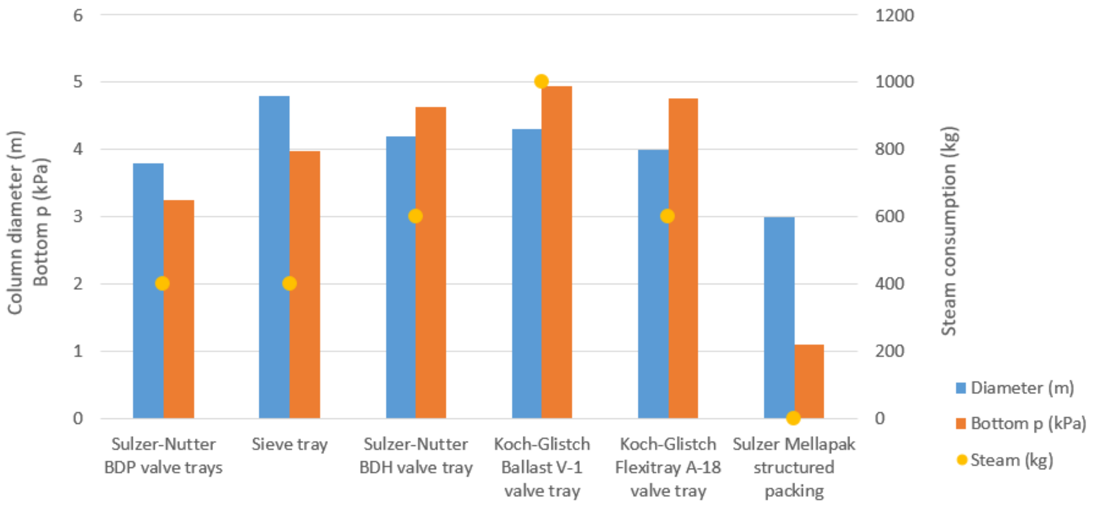

Figure 8.2 Column operations with different internals

The chosen Sulzer-Nutter BDP valve trays were superior compared to other candidates based on simulation results. BDP valve trays achieved the smallest column diameter and pressure drop. Sieve trays required the largest column diameter in order to avoid jet flooding but led to a smaller pressure drop than the other trays. Bubblecap trays were not feasible even with a column diameter of 6 meters. They encountered jet flooding at nearly every stage. Mellapak-structured packing with the packed stage height of 1 m was employed for comparison. It showed a significantly smaller pressure drop of only 1 mbar. Due to minimal pressure loss, the bottom temperature was low and no stripping steam was needed. As the bottom temperature was around 260 °C with trays, it was only about 230 °C with the Sulzer Mellapak-structured packing.

8.1.3 Turndown ratio

One of the most important aspects of the column design is to find out the operating range of distillation apparatus. The hydraulic design that was produced for the base case was analyzed by varying the FFA content of the incoming feed. The FFA yield to the side-stream was kept as 80% of the feed's FFA in all of the turndown simulations. The process constraint was to keep the bottom temperature under 260 °C by injecting stripping steam. The other variables that were adjusted accordingly, were the boilup and reflux ratios and the side-stream and overhead stream sizes. The size of side-stream affects directly the incoming feed's temperature, as it is the heating medium of the preheater, but this just means that the reboiler duty is adjusted accordingly.

The results are presented in Table 8.2. The feed FFA content of the turndown simulations ranged from 90% to 20%. The separation process becomes more difficult when the feed is heavier. This means that the column bottom temperature rises over 260 °C and more stripping steam is needed in order to lower the mixture’s boiling point at the column bottom. In the most difficult case, where the feed FFA content was only 20%, the diameter of the column top stages becomes a limiting factor as a very large amount of steam is needed to lower the bottom temperature, thus increasing the overhead load. In this case, it was not possible to achieve 80% FFA yield to the side-stream and keep the bottom temperature under 260 °C. Stripping steam was not needed when the FFA content of the feed was high enough (≥ 65% FFA). At very high feed FFA content, higher FFA yield is possible without stripping steam. This would require operating at the extreme limits of the column. Reflux should be adjusted as low as possible so that the lower stages would be operated near the weeping limit. At the same time, the top stages would be near the jet flood limit. Operating at the column limits with feeds containing over 80% FFA, it is possible to achieve a side-stream FFA yield of over 90% without injection of steam. It is also noteworthy that with a lower feed FFA content, the simulated side-stream purity drops slightly. This is challenging to alter because raising the reflux ratio also raises the bottom temperature. Then either more steam is needed or the side-stream FFA yield must be reduced.

Table 8.2 Turndown simulation results extracted from Aspen Plus

FFA in feed (%)	90	80	65	40	30	20
FFA yield as side-stream (whole feed) (%)	72	64	52	32	24	16
Side-stream FFA purity (%)	99.997	99.995	99.993	99.989	99.986	99.981
Bottom stream glyceride purity (%)	30.8	53.5	79.5	88.6	92.6	95.8
Bottom stream (glycerides) size (whole feed) (%)	25.2	33.2	49.2	65.2	73.2	81.2
Specifications						
Liquid/vapor ratio	0.21	0.22	0.25	0.31	0.34	0.36
Steam injection (kg)	0	0	0	600	1200	2000
Column results						
Condenser duty (MW)	2.6	2.4	2.2	1.8	1.6	1.5
Reflux ratio	22	21	19	8	5	3
Bottom temperature (°C)	244	247	254	259	260	262
Reboiler heat duty (MW)	4.78	4.62	4.44	4.49	4.50	4.53
Boilup ratio	3.8	2.6	1.7	0.9	0.7	0.6
Preheater duty (MW)	1.07	1.05	1.02	0.56	0.39	0.23
Feed temperature (°C)	120	120	120	95	85	75

Operating the column with a lower feed FFA content is also much more costly as the side-stream is significantly smaller than with higher feed FFA content, while the energy requirement of the reboiler is practically the same. At higher feed FFA content, heat integration is naturally better as a larger portion of the reboiler's heat can be reused in preheating. In addition, steam production raises the operating costs even more as an increased amount of stripping steam is needed to control the bottom temperature.

The bottom stream's glyceride purity rises heavily, when the feed FFA content is lower. From the FAME production perspective, the best separation efficiency is on the low feed FFA contents, as the transesterification process becomes problematic with high FFA content raw materials.

In theory, the same column design could be safely operated at under 10% feed FFA content by increasing the reflux. At very low feed FFA contents, careful analysis has to be done about the potential losses due to thermal decomposition as the simulated bottom temperature rises over 270 °C.

8.1.4 Stream properties

Three types of impurities were present in the simulations (side-stream distillation concept base case results analyzed here): Heavy organochlorides, light organochlorides and VOCs. As expected, VOCs ended up in the overhead stream. The total amount of VOCs in the FFA fraction was about 2 ppm of the stream's weight.

The light organochlorides were also nearly fully vaporized into the overhead stream leaving about 1.8 ppm in the FFA fraction. The value is unrealistically high as the chlorides are often in the form of esters. In refined seed oils, the ratio between bound and free 3-MCPD chlorides is over 30 and can even be as high as 274 [110]. The same ratio in the simulations is now 2. The amount of pure chlorine in the FFA fraction from the light 3-MCPD component in the simulations is about 0.2 ppm. The heavy organochlorides, including 3-MCPD monopalmitin and 3-MCPD dipalmitin stayed at the bottom stream. The FFA fraction only contained about 0.6 ppm of 3-MCPD monopalmitin. The amount of pure chlorine in the FFA fraction from the 3-MCPD monopalmitin was under 0.1 ppm.

The side-stream also contained about 22 ppm of water and monoglycerides. The amounts of monopalmitin and mono-olein were 47 ppm and 12 ppm. In practice, the FFA fraction was free from di- and triglycerides in the base case simulation of the side-stream concept.

The bottom stream consisted mainly of glycerides but also included about 20.5% FFA. Practically all the bound 3-MCPD stayed at the bottom covering about 96 ppm of the bottom stream's mass.

The FFA distribution in different streams is presented in Table 8.3. The results are logical as the bottom stream has the heaviest FFA profile, while the overhead stream has the lightest.

Table 8.3 The FFA profiles of the streams

FFA	Bottom stream (%)	Side-stream (%)	Overhead stream (%)
C6:0A	0.0	0.0	2.3
C8:0A	0.0	0.0	11.3
C10:0A	0.0	0.0	9.7
C12:0A	0.2	0.9	73.3
C14:0A	0.4	1.7	2.3
C16:0A	25.9	46.0	1.0
C18:0A	6.6	4.0	0.0
C18:1A	54.6	37.8	0.0
C18:2A	12.4	9.6	0.0

8.1.5 Column pressure

Kleiber [57] summarizes the influence of pressure on distillation process well: “The higher the column pressure is, the lower are the volume flows. Therefore, higher pressure results in a higher capacity of the column. On the other hand, higher pressure usually (not always) results in a worse separation behavior due to the phase equilibrium, and therefore to a worse separation performance.” Naturally, this also means that vacuum distillation requires larger column diameter as the volume flows are higher. The vacuum’s influence is emphasized in the distillation process covered by this thesis where the gas mass flow is approximately four times bigger than liquid mass flow on the lower stages.

The low pressure is a necessity in lipid fractionation as it also lowers the boiling point of the feed. Without the implementation of a deep vacuum, the distillation feed would be partly thermally decomposed, as stated earlier.

The effect of the column pressure was studied by varying the overhead pressure and scaling the column diameter and side-stream draw-off accordingly. Column diameter and yield have been chosen so that when the column is operated at its hydraulic limits, the bottom temperature is around 260 °C. This would mean that the column cannot be reliably operated at higher temperatures. Feed composition and the amount of stripping steam were kept the same as for the base case simulation. The results are presented in Figure 8.3.

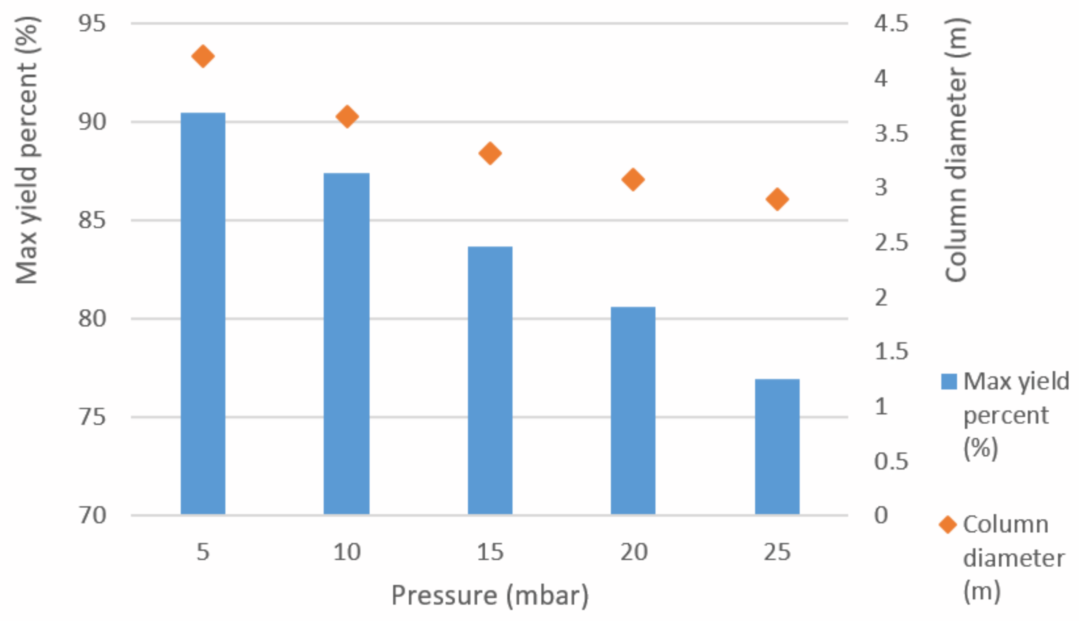

Figure 8.3 Pressure's influence on column diameter and FFA yield

It is clearly seen that there is a strong correlation between the column pressure and the maximum achievable FFA yield to the side-stream. The deeper vacuum also widens the operating range of the column at lower FFA contents as the bottom temperature is lower. The drawback is that a larger column diameter is needed at lower pressures. The creation of higher vacuum also requires more expensive equipment and larger amount of steam for the ejectors. According to Aerstin *et al.* [114], the minimum practical absolute pressure that can be achieved with a two-stage steam ejector system with barometric intercondensers is 5 mm Hg (about 6.7 mbar). A three-stage ejector system with barometric intercondensers consumes, however, less steam at lower, under 30 mm Hg (about 40.0 mbar) pressures, which is probably a better choice. An additional small condenser (~ 60 kW) was added before the ejectors in order to condensate remaining free fatty acids from the overhead stream. In the side-stream column base case, the amount of condensate was about 13% of the overhead stream. The amount of air leakages to the vacuum system was estimated with the help of Table 8.4 as presented by Kleiber [57]. The estimated air leakage rate was approximately 20 kg/h.

Table 8.4 Recommended values for leakage rates [57]

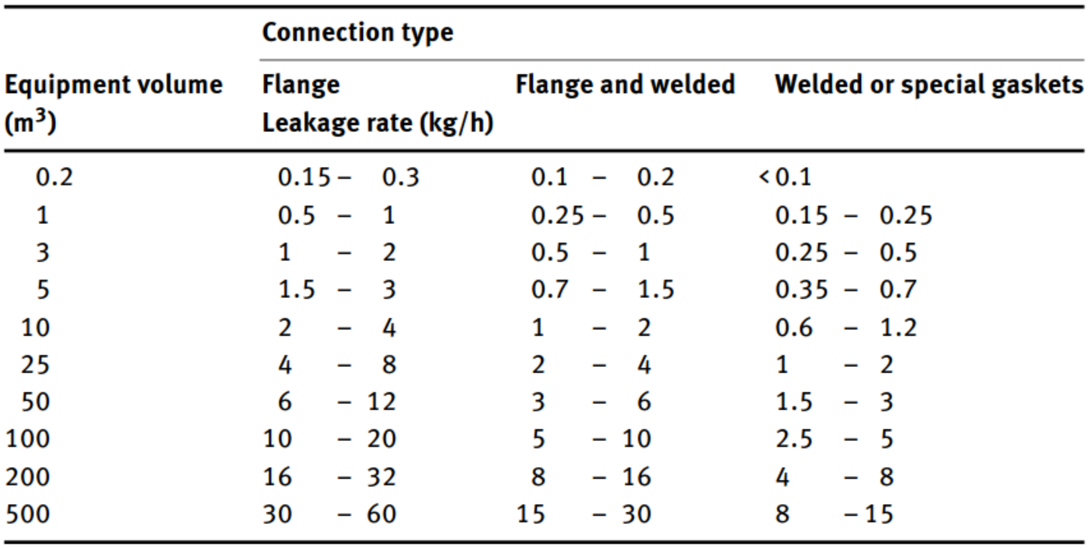

	Connection type		
Equipment volume (m^3)	**Flange** **Leakage rate (kg/h)**	**Flange and welded**	**Welded or special gaskets**
0.2	0.15 – 0.3	0.1 – 0.2	< 0.1
1	0.5 – 1	0.25 – 0.5	0.15 – 0.25
3	1 – 2	0.5 – 1	0.25 – 0.5
5	1.5 – 3	0.7 – 1.5	0.35 – 0.7
10	2 – 4	1 – 2	0.6 – 1.2
25	4 – 8	2 – 4	1 – 2
50	6 – 12	3 – 6	1.5 – 3
100	10 – 20	5 – 10	2.5 – 5
200	16 – 32	8 – 16	4 – 8
500	30 – 60	15 – 30	8 – 15

Steam consumption of the three-stage ejector system was roughly estimated with the help of Figure 8.4. The figure shows the required amount of steam for different ejector systems, having different suction pressures. The overhead stream of the simulations is nearly only steam and the desired vacuum is 10 mbar (7.5 mm Hg). The suction pressure and composition result to a factor of 3.5 which is obtained from Figure 8.4. This means that the steam consumption of the ejector system becomes roughly 3400 kg/h. The actual steam consumption of the ejector system should be discussed with a vendor as Figure 8.4 is from the 1970’s, meaning it is rather old. [114]

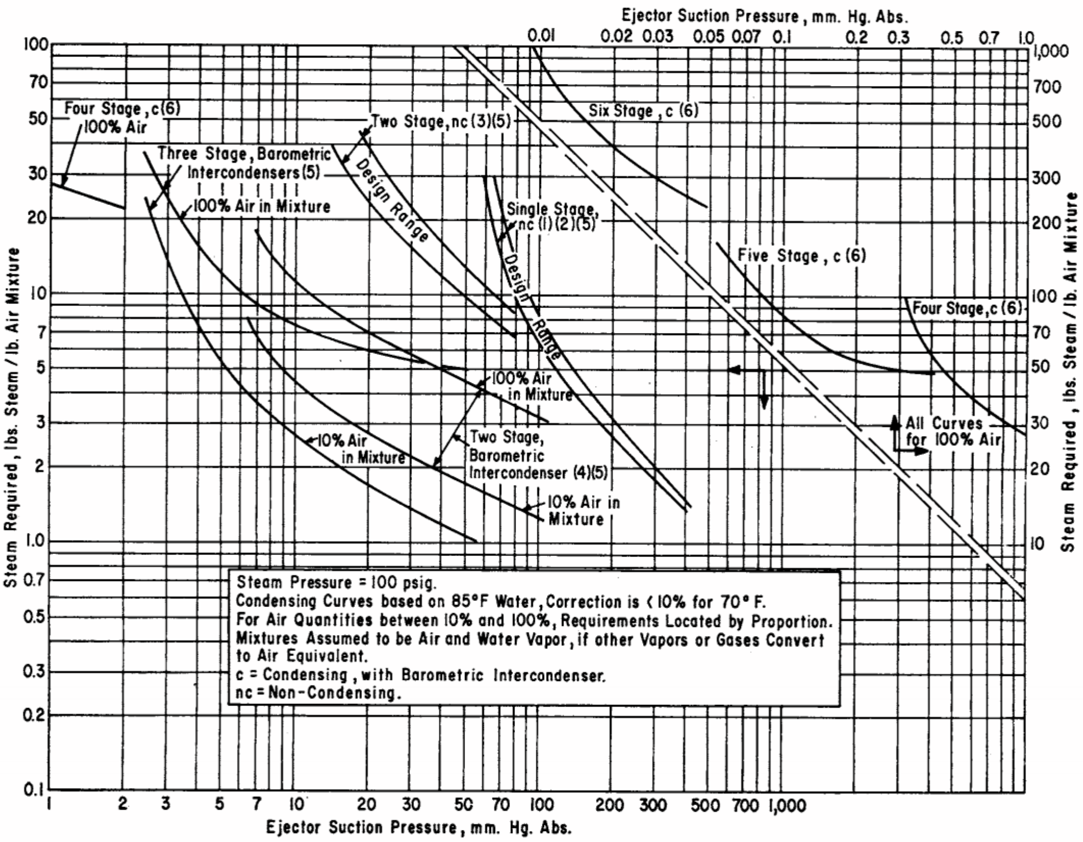

Steam Pressure = 100 psig.
Condensing Curves based on 85°F Water, Correction is < 10% for 70° F.
For Air Quantities between 10% and 100%, Requirements Located by Proportion.
Mixtures Assumed to be Air and Water Vapor, if other Vapors or Gases Convert to Air Equivalent.
c = Condensing, with Barometric Intercondenser.
nc = Non-Condensing.

Figure 8.4 Steam consumption of different ejector systems [114]

8.1.6 Operating costs

The operating costs calculated in this thesis, cover only the utility costs meaning that raw material, operating labor or maintenance expenditures are not estimated. CAPEX is neither calculated. Clearly the largest utility costs result from the hot oil circulation for the reboiler and steam consumption of the ejector system. Other utility costs derive from pump electricity consumption and the possible usage of stripping steam.

It was decided that the reboiler heat demand would be satisfied by consuming natural gas as fuel for the process furnace. A five year average price of natural gas in the EU was calculated to be 3.73 cnt/kWh with the help of official EU statistics [115]. In Finland, the price would be over 6 cnt/kWh due to higher taxation. A typical combustion process efficiency of 0.8 was used for the furnace and an efficiency factor of 0.95 was applied to take heat losses from piping, etc. into account [116]. The equation for expenditures of reboiler becomes:

$$C_{reboiler}\left(\frac{€}{h}\right) = C_{fuel}\left(\frac{€}{kWh}\right) * P_{reboiler}\;(kW)/\;\mu_{tot} \qquad (5),$$

where $C_{reboiler}$ is the reboiler usage cost, C_{fuel} is the fuel price, $P_{reboiler}$ is the reboiler duty and μ_{tot} is the overall efficiency.

The same natural gas price was also used in steam generation cost calculations. A boiler efficiency of 0.95 was used [117]. Enthalpies of boiler feed water and generated steam were read from a pressure-enthalpy diagram for water, presented in Figure 8.5 [118]. The generated, saturated steam's enthalpy is about 2750 kJ/kg at around 15 bar and 200 °C. The feed water's temperature was estimated to be around 20 °C translating to roughly 100 kJ/kg, which was used in calculations. The equation for expenditures of steam generation with boiler becomes:

$$C_{steam}\left(\frac{€}{h}\right) = C_{fuel}\left(\frac{€}{kWh}\right) * (h_s - h_w)\,\frac{kJ}{kg} \,/\, 3600 * m_s\left(\frac{kg}{h}\right) / \,\mu_{boiler} \quad (6),$$

where C_{steam} is the cost of steam, h_s and h_w are the enthalpies of steam and water, m_s is the mass of steam and μ_{boiler} is the boiler efficiency [119].

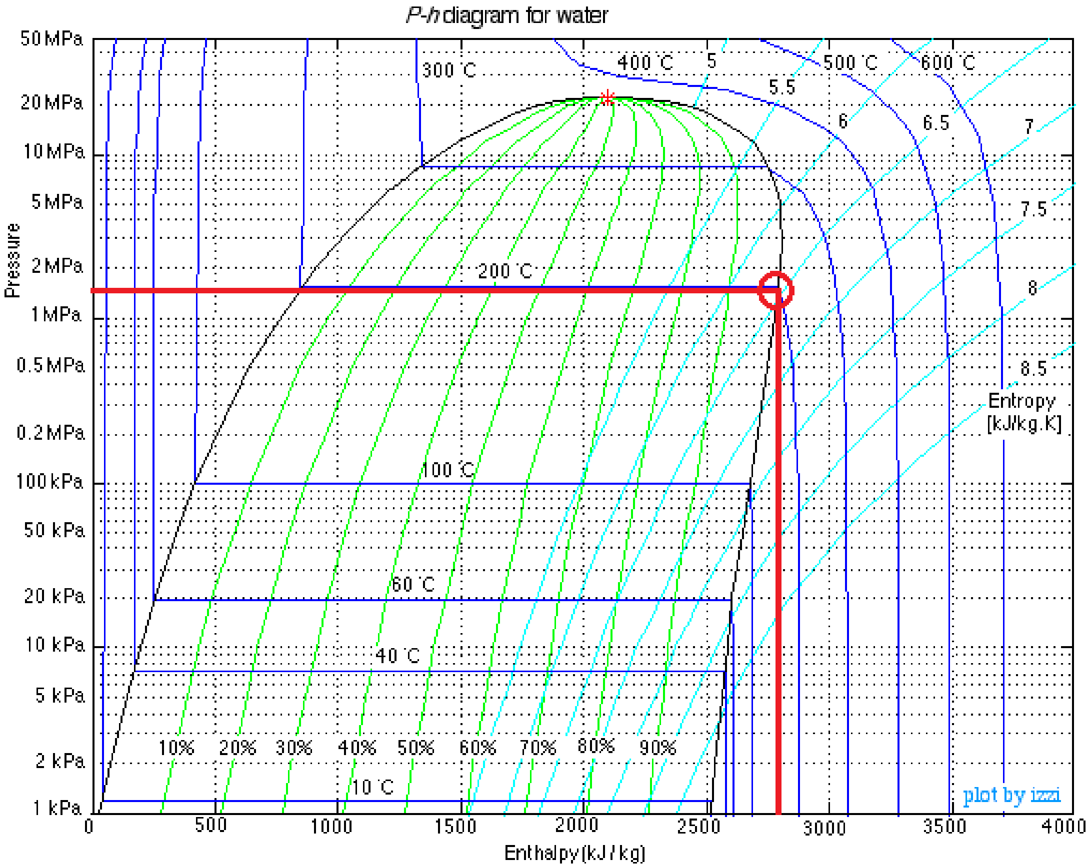

Figure 8.5 Pressure – enthalpy diagram for water [118]

Feed pump, side-stream pump and bottom pump duties were directly used as simulated with the Aspen Plus pump model with default settings and discharge pressures of 5 bar. The amount of cooling water needed for the column condenser was estimated with the help of Aspen's utility calculator. The inlet temperature of feed water was set to 20 °C and the outlet temperature to 60 °C. The cooling water network's pressure was set to 5 bar. Coolers for side-stream (after preheating) and bottom stream also require cooling water. When their cooling duties are known, the required amount of cooling water was calculated by hand with the following energy balance:

$$m\ (kg)\ = \frac{P\ (kW)*3600\ (\frac{s}{h})}{C_p\left(\frac{kJ}{kg*{}^{\circ}\mathrm{C}}\right)*(T_2 - T_1)({}^{\circ}\mathrm{C})} \qquad (7),$$

where m is the mass of required cooling water, P is the cooling duty of a cooler, C_p is the heat capacity of water and T_2 and T_1 are cooling water temperatures after and before the cooler [120]. The same cooling water temperatures were used in the calculations that had been implemented in Aspen Plus. Water's heat capacity is relatively constant between 20 °C and 60 °C and the value of 4.18 kJ/(kg * °C) was chosen [121]. The amount of cooling water for the condenser and the coolers was summed up and a corresponding pump effect was calculated in Aspen Plus.

The steam need for the ejectors is calculated as explained in the section 8.1.5. The needed cooling water for the second condenser before the ejector system is calculated with equation 7 and added to the Aspen's cooling water pump calculation.

Calculated utility costs are presented in Figure 8.6. Costs were calculated for the same cases that were simulated in the section 8.1.3. In all the simulations, an FFA yield to the side-stream of 80% was obtained and the bottom temperature was kept around 260 °C.

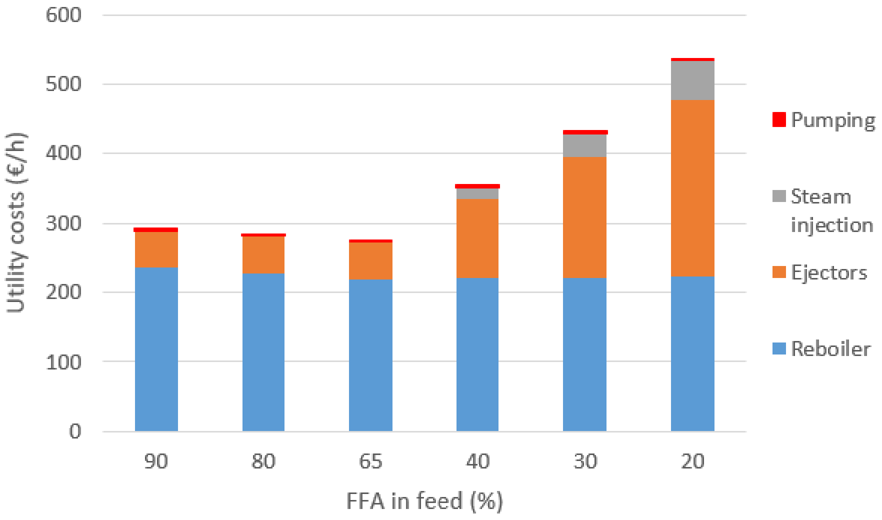

Figure 8.6 Utility costs of the side-stream column concept

The pumping costs were approximately the same in all the cases, about 3.5 €/h. The reboiler costs were the highest at 90% feed FFA content (235 €/h) and the lowest at 65% feed FFA content (218 €/h). The reboiler costs remained at 220 €/h between 40% and 20% FFA content. The relatively high reboiler costs at lower FFA content result from the less efficient heat integration and the heavier feed. As the enthalpy of the side-stream is lower, the preheating is not as effective and the feed has a lower temperature when it enters the column. This, combined with the heavier feed composition, results in the elevated reboiler duty. Steam injection to the column affects directly the overhead operations as the amount of uncondensable fluid entering the ejectors is also increased. This means that a larger amount of motive fluid (steam) is also needed to pull the vacuum. It should be further studied how thermal decomposition occurs in distillation conditions for a certain fat feedstock and if steam is actually needed. There is also a possibility to condense the whole overhead stream, but it would need a very low temperature of about 5 °C at the specified pressure. By condensing the whole overhead stream, the ejector steam consumption would drop dramatically but this would require additional cooling equipment and utility. The steam costs would not be as significant an issue if heat integration of bottom stream for steam generation is implemented. The heat integration would cut a large portion of the operating costs at the lower FFA content.

8.2 Pre-flash and simple column concept base case results

In the pre-flash concept, the feed composition was the same as in the side-stream base case simulation. The same column internals with the same modifications as in the side-stream distillation column were applied to the simple distillation column. The simulated column diameter for this case was 3.5 m, while tray spacing was maintained at 0.91 m. The resulting column height would become only about 3.7 m. The geometry of the column becomes rather unconventional as the column's diameter is practically equal to its height. No literature references about such columns were found and the geometry should be further investigated and discussed with a vendor if such a concept would be implemented.

The complete pre-flash concept base case simulation results are presented in Table 8.5. A yield of 86.2% of the feed's FFA is received as an overhead stream from the simple distillation column. The overhead stream purity was almost 99.99% including 5 ppm of the lightest 3-MCPD and 36.1 ppm VOCs. The reboiler heat duty was about 4.0 MW and the bottom temperature stayed just below 260 °C. The condenser duty was 0.9 MW while the reflux ratio was 0.6. The reflux ratio could have been separation-wise lower but it was maintained at 0.6 in order to avoid column drying.

Table 8.5 Pre-flash concept base case simulation results

BASE CASE RESULTS	
FFA yield as an overhead stream (%)	86.2
Overhead stream size (%)	56.0
Overhead stream FFA Purity (%)	99.988
Bottom stream size (%)	41.2
Bottom stream glyceride purity (%)	79.5
Specifications	
Liquid/vapor ratio at the bottom separation stage	0.24
Pre-flash results	
Feed temperature (°C)	140
Percentage of the feed flashed (%)	2.8
Column results	
Condenser duty (MW)	0.9
Reflux ratio	0.6
Bottom temperature (°C)	259
Reboiler heat duty (MW)	4.0
Boilup ratio	3.8
Preheater duty (MW)	1.4
Feed temperature (°C)	140

The pre-flash distillation concept requires an additional heating source for the feed if it contains a low amount of FFA. The overhead stream is used to pre-heat the feed and if the overhead stream is small enough, not enough heat is available to raise the feed's temperature to 140 °C. In practice, if the concept is operated with feedstocks containing less than 40% FFA, an external heating source would be needed. In theory, a feed with 30% FFA would be sufficient, but then the required exchanger area would become over 40 m^2. The bottom temperature of the pre-flash concept also exceeds the preferred 260 °C limit at feedstocks with a feed FFA content of under 50%, if 80% FFA yield to the overhead stream is demanded. Operating the column at high, over 80% feed FFA-content is also problematic. The top tray of the column approaches the jet flood limit. The problem could be solved by lowering the reflux ratio but, on the other hand, this would lead to other problems such as too low liquid flow inside the column. Another solution could decreasing the number of valves per active area of the trays to Aspen's default 75. This would, however, increase the bottom temperature and limit the operability at lower feed FFA contents.

The operating costs at varying feed FFA contents are presented in Figure 8.7. In all the simulations, a feed FFA yield to the overhead stream of 80% was obtained. Bottom temperature was kept under 260 °C in all the simulations except the one where feed FFA content was 40%. In this case, temperature rose nearly to 270 °C. The main operating cost derived from the reboiler usage. The ejector steam usage was the same in every case. The pumping costs are slightly higher at lower feed FFA contents.

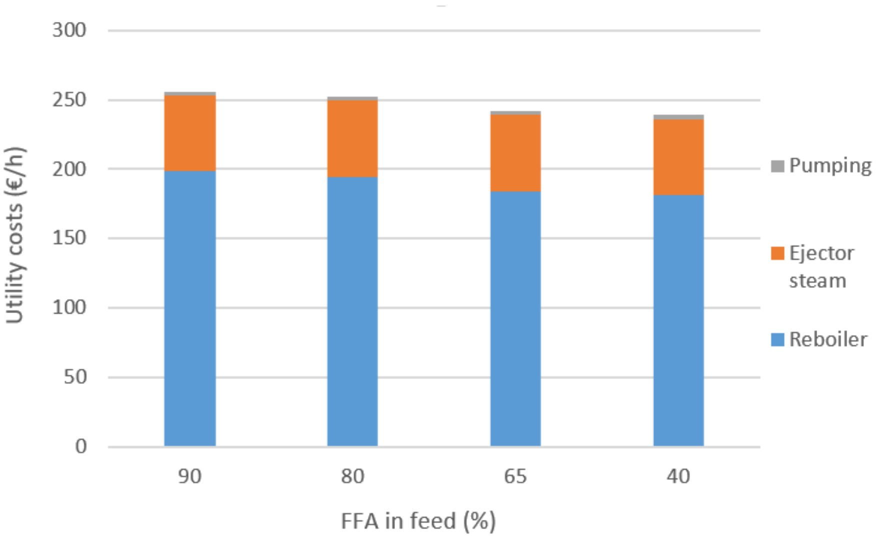

Figure 8.7 Utility costs of the pre-flash distillation concept

8.3 Heat integration

It is common practice to utilize the heat of product streams in either preheating of the feed or other purposes on site (e.g. steam generation or heating of other streams on site). The main interest on this distillation case is the heat utilization of the FFA fraction.

The FFA fraction is drawn from the process at over 220 °C. The fraction contains no remarkable amounts of either light or heavy impurities. VOCs have been distilled to the overhead and heavies stay at the bottom stream, meaning that the stream should not be too fouling for heating service. In the side-stream concept base case, FFA fraction can be successfully utilized to preheat the feed stream from 60 °C to 120 °C. Aspen’s HeatX countercurrent model was used to give an approximation of the heat exchanger details. Detailed exchanger geometry calculations were not performed as the shortcut model was considered to give informative results. The preheating requires an exchanger area of 13.7 m^2 with the heat duty being close to 1 MW.

The feed has a kinematic viscosity of approximately 12.1 centistokes (cSt) and temperature of 60 °C. The heating medium has a temperature of over 200 °C. As the viscosity is not especially high, but the temperatures are considerable, shell and tube exchanger (STHE) could be chosen. Gasketed plate heat exchanger (PHE) should be considered If the viscosities are considered too high for STHE by the vendor or the operations are changed so that temperature or pressure are lower. As the feed may be fouling, a removable tube bundle should be used for the STHE. Spiral plate heat exchanger (SPHE) should be considered if there is a possibility for a high solids content. [23]

The quantity and temperature of overhead stream are quite low in the side-stream column base case, which means that it is not worth integrating the stream at least for the preheating purposes of the feed. The bottom stream of distillation process would be a great source of heat as the stream is quite large and has a temperature around 260 °C. The stream is, however, not integrated to process as its composition may be uncertain if all relevant components are not included in the simulation. The viscosity of bottom stream is larger than the side-stream's and may be larger than the simulation results predict. The simulation does not take into account the possible polymerization and the consequential accumulation of oligomers in a fat feedstock. Also, depending on the feed origin, a high amount of inorganic matter and solid particles may accumulate to the bottom stream making it seriously fouling and challenging substance for heat exchangers.

Heat integration of bottom stream has been partly tested in the pre-flash concept as was suggested by Professor R. Zevenhoven of Åbo Akademi University. Here, the bottom stream is used to heat the FFA fraction. The goal is to ensure that the FFA fraction is warm enough to heat the feed to 140 °C before the flash drum. The temperature of the FFA fraction, which is 100% vapor when drawn off, is raised by 10-15 °C. The simulated viscosity of bottom stream is still quite low at the higher, over 200 °C, temperatures and would not be as problematic. The bottom stream's heat could also be utilized to some extent in the side-stream concept. The liquid FFA fraction would be pumped through the heat exchanger and its temperature would be raised by 10-15 °C. Here, a larger heat recovery is achieved with the feeds that contain a lower amount of free fatty acids and the bottom stream is larger.

Another way to integrate the heat of bottom stream would be to use it in steam generation. This would result in significant energy savings as discussed later in the section 8.1.6. This heat integration was tested successfully with the base case values. In the side-stream concept base case, a steam generator was added to the bottom of the column. The bottom stream was used as a heating medium while a water stream at 20 °C and 15 bar was added to the cold side of the steam generator. At the side-stream column concept base case, a steam injection of 400 kg was needed in order to keep the bottom temperature of the column under 260 °C. The steam was generated while maintaining a bottom stream temperature of 218 °C after the steam generator. The required heat exchanger area became 3.1 m^2 and the heat duty was 306 kW. The same questions regarding serviceability of the bottom stream remain, as the stream might be too fouling for heat exchange duty.

Temperature of the incoming feed did not have a remarkable effect on the distillation process. This means that all the available, economically usable heat should be integrated to the preheat train as long as the inlet temperature is lower than the bottom temperature. Every stream was eventually cooled to 60 °C. This means that there are definitely further considerations for heat integration if such a concept would be executed.

8.4 Comparison between the studied concepts

The pre-flash concept has not been analyzed in depth as the main focus of this thesis is on the side-stream distillation concept. This chapter, however, provides a short comparison between the two concepts. The main differences between the concepts are summarized in Table 8.6.

Table 8.6 Summary of the main differences between the concepts

Attribute	Side-stream distillation column concept	Pre-flash and simple distillation column concept
Energy consumption	0.7 MW Higher. Mostly because the FFA fraction is condensed and drawn from the column in liquid form.	0.7 MW Lower. The FFA fraction is drawn as vapor. The preheating of the feed is more effective which lowers the reboiler energy demand.
Operating costs	276 €/h at base case.	242 €/h at base case.
Turndown ratio	Better. No hydraulic problems when operated at 90%-20% FFA. Steam coupling allows operations at low FFA contents.	Worse. Risk of jet flooding at 90% FFA content. Bottom temperature rises over 260 °C when the feed FFA content is under 50%.
Stream Purity	Better. Separation of the light fraction is more effective. Slightly worse separation of the glyceride/bound 3-MCPD fraction	Worse. Less effective separation of the light fraction. Slightly better separation of the glyceride/bound 3-MCPD fraction
Column internals and geometry	Larger column diameter (3.8 m) and more separation stages (6).	Smaller column diameter (3.5 m) and less separation stages (3).

Energy-wise, the pre-flash concept is a better alternative compared to the side-stream column concept. Energy consumption of the reboiler is about 0.7 MW lower in the pre-flash concept. There are a couple of reasons for this. First of all, as the FFA fraction is in vapor form in the pre-flash concept, there is more heat available for preheating and other heat integration targets in the form of latent heat. The heat of the FFA fraction should be utilized so that the stream is fully condensed. Otherwise, cooling water has to be employed, so that the FFA fraction does not end up in the ejectors. The bottom pressure of the pre-flash concept is also lower, which means that less heating is needed to vaporize the feed. Part of the feed is also flashed before entering the column. Overhead operations of the side-stream concept are also more energy-demanding. The FFA fraction is drawn off from the side-stream column in liquid form which causes about 1.5 MW extra condenser duty. The condenser duty at the simple distillation column is only about 1 MW while it is 2.5 times higher in the side-stream column. Cooling is, however, significantly less costly than heating.

As there are twice the number of trays in the side-stream column than in the simple distillation column, the bottom pressure is higher than in the simple distillation column and steam is required to lower the process fluid's boiling point by reducing the bottom temperature to below 260 °C. 86.1% feed FFA yield to the overhead stream is obtained from the pre-flash concept without a steam injection, as 400 kg is needed in the side-stream distillation concept to achieve the same FFA yield to the side-stream and maintain temperatures below specification.

The side-stream concept provides better turndown and more flexible operability than the pre-flash concept. If the feed is heavier and contains less free fatty acids, the bottom temperature can be controlled by adding steam. The concept with a pre-flash drum has a limited operating range and cannot be operated with under 50% feed FFA content if the bottom temperature is desired to be kept under 260 °C. The column hydraulics shift close to a weeping limit as the overhead draw-off is smaller. Increasing the amount of reflux fixes the issue but on the other hand raises the bottom temperature over 260 °C. In theory, steam coupling could be applied also to simple distillation column, but then another separation would be needed if water is desired to be removed from the FFA fraction. This would mean a construction of another flash drum downstream of the column. Operating the pre-flash concept at higher feed FFA contents becomes difficult as the top tray approaches the jet flood limit.

If operations are allowed to continue at over 260 °C and the temperature limit would be, for example 300 °C, the pre-flash concept's operability would be more feasible. In this case, the column can be operated at about 20% feed FFA content with an overhead FFA yield of 80%. In order to achieve operability at 20% feed FFA content, tray modifications regarding the number of valves per active area must be restored to Aspen's default value of 75 to avoid weeping which would occur otherwise. Even with the mentioned change, 20% feed FFA is the lower limit for pre-flash concept as the bottom temperature is then around 300 °C.

The pre-flash concept also requires a high enough feed temperature before the flash drum whereas the feed temperature of the side-stream concept does not offer more than saving heat energy. This means that the FFA fraction in the pre-flash concept has to be large enough, or otherwise additional preheating arrangements are needed. For example, in the case where feed contains only 20% FFA, the overhead stream would not be large enough to provide a necessary amount of heat to pre-flashing.

The FFA fraction purity at the pre-flash concept is compromised as the light compounds are removed in a one-stage separation. The FFA fraction from the pre-flash concept contained over 36.1 ppm VOCs of the final fraction's weight while the side-stream column concept only contained 2 ppm. The FFA fraction from the pre-flash concept also contained more free 3-MCPD (5.3 ppm) than the FFA fraction from side-stream column (1.8 ppm). The pre-flash concept succeeded better than side-stream column concept in the separation of heavier compounds between the bottom and overhead streams. The pre-flash concept FFA fraction contained less bound 3-MCPD (0.2 ppm) and glycerides than the side-stream column concept FFA fraction.

The operating costs of the concepts were compared. Both concepts were simulated with the base case feed so that the FFA recovery to overhead or side-stream was 80% of the feed's FFA. This means that the steam injection to the side-stream column was not needed. The total operating costs of the side-stream column concept were about 276 €/h while the expenses of the pre-flash concept were about 242 €/h. This means that with the feed containing about 65% FFA, the pre-flash concept's utility costs are about 34 €/h lower.

9 Conclusions

Two distillation concepts for the separation of free fatty acids from fat or oil feedstocks were introduced, analyzed and simulated. The main focus was on a concept including a side-stream column which was studied and developed in detail. The other concept included a pre-flash drum and a simple distillation column. The developed concepts and their process conditions are influenced by the findings presented in the literature part of this thesis.

The side-stream distillation concept simulations showed that only a few separation stages are needed to separate the FFA fraction from the glyceride fraction in a fat feedstock. According to the turndown ratio simulations, the side-stream column can be reliably operated at varying feed FFA contents between 90% and 20%. At lower feed FFA content, the rising bottom temperature can be controlled by adding steam. An FFA yield of over 80% of the feed's FFA was achieved for varying feed FFA content. The operating costs of the concept rise heavily if steam is injected. If the feed FFA content and the consequent side-stream mass flow are low enough, the costs also rise because of the less efficient heat integration.

The pre-flash distillation concept also returned promising results. The separation of light components was not as effective as in the side-stream concept, but, on the other hand, the FFA distillate was cleaner from heavier compounds. The purity of glyceride fraction was about the same as in the side-stream column concept. As the distillation column in the pre-flash concept has fewer trays than the side-stream column, the pressure drop is also lower. This leads to a lower bottom temperature and reduced reboiler costs. At lower feed FFA content, the bottom temperature can still rise over 260 °C in the pre-flash distillation concept. If steam were applied, an extra separation after the column would also be needed. The operating costs of the pre-flash distillation concept were lower than those of the side-stream column concept.

Both of the concepts show promising simulation results. The simulation results suggest that both of the distillation concepts give a good separation of the FFA and glyceride fractions. The glyceride purity of the bottom fraction is not quite good enough, even at the low feed FFA contents, for the FAME production, but its purification could be further studied. Both of the distillation concepts could also handle varying amounts of FFA in the feed. The produced results describe process conditions in which the concepts should be operated and the reasoning behind them. The methodology behind choosing the right column internals and geometry was also covered. Because of the required deep vacuum, the simulated column diameter of both concepts becomes quite large. The deeper vacuum, however, enables better separation between the FFA and glycerides and provides a wider operating range of the column. The pressure of the concepts could be set lower than 10 mbar, which was employed in the simulations. The choice of internals also has a large impact on the required column diameter and the pressure drop. Due to the possible fouling tendency of waste fat feedstock, trays were employed in the simulations. Structured packing should be employed if possible, because of the superior properties compared to trays.

There are, however, issues that need to be investigated before further development of the concepts. The potential fouling of the feed is an unknown factor and heavily depends on the origin and type of the feed. The fouling nature of the feedstock affects the required pre-processing methods and the column internals that will be chosen. The valve trays that were applied in the simulations may not be feasible for the process because of the potential fouling. It is also important to find out if the bottom stream can be utilized, for example, in the steam generation or if it is too fouling. Thermal degradation and oligomerization of the feedstock should also be further investigated. Based on that, the precise maximum bottom operating temperature can be chosen. The column geometry is also uncertain and should be discussed with a vendor. The column reflux is also set unnecessarily high (from the separation point of view) in order to avoid drying, which promotes energy inefficiency.

References

[1] Owen, N. A., Inderwildi, O. R., & King, D. A. (2010). The status of conventional world oil reserves—Hype or cause for concern? *Energy Policy, Volume 38*(Issue 8), 4743-4749.

[2] Shafiee, S., & Topal, E. (2009). When will fossil fuel reserves be diminished? *Energy Policy, 37*(1), 181-189.

[3] BP. (2019, September 13). *Statistical Review of World Energy*. Retrieved from Statistical Review of World Energy: https://www.bp.com/en/global/corporate/energy-economics/statistical-review-of-world-energy/oil.html#oil-reserves

[4] Kalnes, T. N., Koers, K. P., Marker, T., & Shonnard, D. R. (2009). A Technoeconomic and Environmental Life Cycle Comparison of Green Diesel toBiodiesel and Syndiesel. *Environmental Progress & Sustainable Energy, 28*, 111-120.

[5] Tsouko, E., Papanikolaou, S., & Koutinas, A. (2016). Production of fuels from microbial oil using oleaginous microorganisms. In *Handbook of Biofuels Production (Second Edition)* (pp. 201-236). Woodhead Publishing.

[6] Marchetti, J. M. (2010). Biodiesel Production Technologies. In J. M. Marchetti, *Biodiesel Production Technologies* (p. xi). New York: Nova Science Publishers, Inc.

[7] Zhang, Y., Dubé, M., McLean, D., & Kates, M. (2003). Biodiesel production from waste cooking oil: 2. Economic assessment and sensitivity analysis. *Bioresource Technology 90*, 229-240.

[8] Inflation Data. (2019, October 10). *Historical Crude Oil Prices*. Retrieved from Inflation Data: https://inflationdata.com/articles/inflation-adjusted-prices/historical-crude-oil-prices-table/

[9] Chai, M., Tu, Q., Lu, N., & Yang, Y. J. (2014). Esterification pretreatment of free fatty acid in biodiesel production, from laboratory to industry. *Fuel Processing Technology, 125*, 106-113.

[10] Patil, P. D., Gude, V. G., K., R. H., Muppaneni, T., & Deng, S. (2012). Biodiesel Production from Waste Cooking Oil Using Sulfuric Acid and Microwave Irradiation Processes. *Journal of Environmental Protection, 3*, 107-113.

[11] Wang, Y., Ou, S., Liu, P., Xue, F., & Tang, S. (2006). Comparison of two different processes to synthesize biodiesel by waste cooking oil. *Journal of Molecular Catalysis, 252*, 107-112.

[12] Suwanno, S., Rakkan, T., Yunu, T., Paicid, N., Kimtun, P., Prasertsan, P., & Sangkharak, K. (2017). The production of biodiesel using residual oil from palm oil mill effluent and crude lipase from oil palm fruit as an alternative substrate and catalyst. *Fuel, 195*, 82-87.

[13] Hayyan, A., Alam, M. Z., Mirghani, M. E., Hamiki, N. I., Siran, Y. M., & Tahiruddin, S. (2011). Reduction of high content of free fatty acid in sludge palm oil via acid catalyst for biodiesel production. *Fuel Processing Tehnology, 92*, 920-924.

[14] Hayyan, A., Alam, M. Z., Mirghani, M. E., Kabbashi, N. A., Hakimi, N. I., Siran, Y. M., & Tahiruddin, S. (2010). Sludge palm oil as a renewable raw material for biodiesel production by two-step processes. *Bioresource Technology, 101*, 7804-7811.

[15] Ibrahim, A. H., Dahlan, I., Adlan, M. N., & Dashti, A. F. (2014). Using Horizontal Roughing Filter as an Effective Post-Treatment System for Palm Oil Mill Effluent (POME): Effect of Media Sizes and Filtration Rates. *Current Environmental Engineering, 1*, 111-117.

[16] Yunos, K. F., Mazlan, N. A., Naim, M. N., Baharuddin, A. S., & Hassan, A. R. (2019). Ultrafiltration of palm oil mill effluent: Effects of operational pressure and stirring speed on performance and membranes fouling. *Environmental Engineering Research, 24*, 263-270.

[17] Tang, Y., Cui, X., Yuan, H., Shen, M., Li, C., Zou, Y., . . . Cao, Z. (2014). *China Patent No. 105368580A.*

[18] Chen, C.-Y., Wen-Jhy, L., Mwangi, J. K., Wang, L.-C., Wu, J.-L., & Lin, S.-L. (2017). Reduction of Persistent Organic Pollutant Emissions during Incinerator Start-up by Using Crude Waste Cooking Oil as an Alternative Fuel. *Aerosol and Air Quality Research, 17*, 899-912.

[19] Soeriaatmadja, W. (2019, July 18). *Indonesia could halt palm oil shipments to Europe*. Retrieved from The Straits Times: https://www.straitstimes.com/asia/se-asia/indonesia-could-halt-palm-oil-shipments-to-europe

[20] Chhetri, A. B., Tango, M. S., Budge, S. M., Watts, K. C., & Islam, M. R. (2008). Non-Edible Plant Oils as New Sources for Biodiesel Production. *International Journal of Molecular Sciences, 9*, 169-180.

[21] Gunstone, F. D., & Padley, F. B. (1997). *Lipid Technologies and Applications.* New York: Marcel Dekker, Inc.

[22] Noor Lida, H., Sundram, K., Siew, W., Aminah, A., & Mamot, S. (2002). TAG composition and solid fat content of palm oil, sunflower oil and palm kernel olein blends before and after chemical interesterification. *Journal of the AAmerican Oil Chemist's Society, 79*, 1137-1144.

[23] NIST - U.S. National Institute of Standards and Technology. (2019, January 20). *Tripalmitin*. Retrieved from NIST - U.S. National Institute of Standards and Technology Web Site: https://webbook.nist.gov/cgi/cbook.cgi?ID=C555442&Mask=2

[24] PubChem. (2019, January 20). *Palmitic acid*. Retrieved from U.S. National Library of Medicine: https://pubchem.ncbi.nlm.nih.gov/compound/Palmitic-acid

[25] Smith, R., & Jobson, M. (2000). Distillation. In I. D. Wilson, *Encyclopedia of Separation Science* (pp. 84-103). Academic Press.

[26] Santander, C. M., Rueda, S. M., da Silva, N. d., de Camargo, C. L., Kieckbusch, T. G., & Maciel, M. R. (2012). Measurements of normal boiling points of fattyacid ethyl esters and triacylglycerols by thermogravimetric analysis. *Fuel, 92*, 158-161.

[27] Wallek, T., Rarey, J., Metzger, J. O., & Gmehling, J. (2013). Estimation of Pure-Component Properties of Biodiesel-Related Components: Fatty Acid Methyl Esters, Fatty Acids, and Triglycerides. *Industrial & Engineering Chemistry Research*, 16966-16978.

[28] Palanisamy, S., & Gevert, B. S. (2016). Study of non-catalytic thermal decomposition of triglyceride at hydroprocessing condition. *Applied Thermal Engineering, 107*, 301-310.

[29] Nawar, W. W. (1969). Thermal Degration of Lipids. A Review. *Journal of Agricultural and Food Chemistry, 17*, 18-21.

[30] Southard, M. Z., & Rowley, R. L. (2019). Section 2: Physical and Chemical Data. In D. W. Green, *Perry's Chemical Engineers' Handbook 9th edition.* McGraw Hill Education.

[31] Zhang, Q., Saleh, A. S., Chen, J., & Shen, Q. (2012). Chemical alterations taken place during deep-fat frying based on certain reaction products: A review. *Chemistry and Physics of Lipids, 165*, 662-681.

[32] Sánchez-Muniz, F. J., & Bastida, S. (2003). Frying oil discarding: polar content vs. oligomer content determinations. *Forum of nutrition, 56*, 345-347.

[33] Tasioula-Margari, M., Márquez-Ruiz, G., & Dobarganes, M. (1996). Fractionating of Oligomeric Triacylglycerides and the Relation to Rejection Limits for Used Frying Oils. *Journal of the American Oil Chemists' Society, 73*, 1579-1584.

[34] Takeoka, G. R., Full, G. H., & Dao, L. T. (1997). Effect of Heating on the Characteristics and Chemical Composition of Selected Frying Oils and Fats. *Journal of Agricultural and Food Chemistry, 45*, 3244-3249.

[35] FSSAI - Food Safety and Standards Authority of India. (2017, May 08). *Can we re-use cooking oil, once it is utilized for frying foods*. Retrieved from FSSAI - Food Safety and Standards Authority of India Web site: https://foodsmart.fssai.gov.in/reusingoil.html

[36] Bonetti, R., Jr., P., & O., W. (2019). Insights into Polymerization of Vegetable Oil: Oligomerization of Oleic Acid. *Journal of the American Oil Chemists' Society, 96*, 1181-1184.

[37] Choe, E., & Min, D. (2007). Chemistry of Deep-Fat Frying Oils. *Journal of Food Science, 72*, 77-86.

[38] Kim, D.-S., Hanifzadeh, M., & Kumar, A. (2007). Trend of Biodiesel Feedstock and Its Impact on Biodiesel Emission Characteristics. *Environmental Progress & Sustainable Energy, 37*(1).

[39] Haas, M. J. (2010). Alternate Feedstocks Technologies for Biodiesel Production. In M. J. Haas, *The Biodiesel Handbook (Second Edition)* (pp. 47-65). Urbana, Illinois: AOCS Press.

[40] Ghazani, S. M., & Marangoni, A. G. (2013). Minor Components in Canola Oil and Effects of Refining on These Constitues: A Review. *Journal of the American Oil Chemists' Society, 90*, 923-932.

[41] Pryde, E. (1980). Composition of soybean oil. In E. Pryde, *Handbook of soy oil processing and utilization* (pp. 13-31). Peoria, Illinois.

[42] Tou Gee, P. (2007). Analytical characteristics of crude and refined palm oil and fractions. *European Journal of Lipid Science and Technology, 109*, 373-379.

[43] Gui, M., Lee, K., & Bhatia, S. (2008). Feasibility of edible oil vs. non-edible oil vs. waste edible oil as biodiesel feedstock. *Energy*(33), 1646-1653.

[44] Phan, A. N.;& Phan, T. M. (2008). Biodiesel production from waste cooking oils. *Fuel*, 3490-3496.

[45] Kulkarni, M. G., & Dalai, A. K. (2006). Waste Cooking Oil - An Economical Source For Biodiesel: A Review. *Industrial & Engineering Chemistry Research*, 2901-2913.

[46] Broaddus, H. (2017, February 6). *What Does RBD Mean, In Relation To Bulk Oils?* Retrieved from Centra Foods: http://www.centrafoods.com/blog/what-does-rbd-mean-in-relation-to-bulk-oils

[47] Freedman, B., Phyde, E., & Mounts, T. (1984). Variables affecting the yields of fatty esters from transesterified vegetable oils. *Journal of the American Oil Chemists Society, 61*(10), 1638-1643.

[48] Mannu, A., Vlahopoulou, G., Urgeghe, P., Ferro, M., Del Caro, A., Taras, A., . . . Petretto, G. L. (2019). Variation of the Chemical Composition of Waste Cooking Oils upon Bentonite Filtration. *Resources, 8*.

[49] Takeoka, G., Perrino, C., & Buttery, R. (1996). Volatile Constituents of Used Frying Oils. *Journal of Agricultural and Food Chemistry, 44*, 654-660.

[50] Wu, C.-M., & Chen, S.-Y. (1992). Volatile Compounds in Oils After Deep Frying or Stir Frying and Subsequent Storage. *Journal of American Oil Chemists Society*, 858-865.

[51] Kamyab, H., Chelliapan, S., Fadhil MD Din, M., Rezania, S., & Khademi, T. K. (2018). Palm Oil Mill Effluent as an Environmental Pollutant. In *Palm Oil.* Intech Open.

[52] Foo, K., & Hameed, B. (2010). Insight into the applications of palm oil mill effluent: A renewable utilization ofthe industrial agricultural waste. *Renewable and Sustainable Energy Reviews, 14*, 1445-1452.

[53] Hadiyanto. (2013). Phytoremediations of Palm Oil Mill Effluent (POME) by Using Aquatic Plants and Microalge for Biomass Production. *Journal of Environmental Science and Technology, 6*, 79-90.

[54] Habib, M., Yusoff, F., Phang, S., & Ang, K. M. (1997). Nutritional values of chironomid larvae grown in palm oil mill effluent and algal culture. *Aquaculture, 158*, 95-105.

[55] Adewale, P., Dumont, M.-J. D., & Ngadi, M. (2015). Recent trends of biodiesel production from animal fat wastes and associated production techniques. *Renewable and Sustainable Energy Reviews, 45*, 574-588.

[56] Nebel, B. A., & Mittelbach, M. (2006). Biodiesel from extracted fat out of meat and bone meal. *European Journal of Lipid Science and Technology, 108*, 398-403.

[57] Kleiber, M. (2016). *Process Engineering Addressing the Gap Between Study and Chemical Industry.* Bad Soden: De Gruyter.

[58] Li, X., Wu, B., & Zhu, J. (2018). Hazards of Organic Chloride to Petroleum Processing in Chinese Refineries and Industrial Countermeasures. *Progress in Petrochemical Science, 2*(3), 1-4.

[59] Gutzeit, J. (2000). Effect of Organic Chloride Contamination of Crude Oil on Refinery Corrosion. *CORROSION*, 26-31.

[60] Sidibé, S., Blin, J., Vaitilingom, G., & Azoumah, Y. (2010). Use of crude filtered vegetable oil as a fuel in diesel engines state of the art: Literature review. *Renewable and Sustainable Energy Reviews 14, 14*, 2748-2759.

[61] Issariyakul, T., Kulkarni, M. G., Dalai, A. K., & Bakhshi, N. N. (2007). Production of biodiesel from waste fryer grease using mixed methanol/ethanol system. *Fuel Processing Technology, 88*, 429-436.

[62] Sudhir, C., Sharma, N., & Mohanan, P. (2007). Potential of Waste Cooking Oils as Biodiesel. *Emirates Journal for Engineering Research, 12*, 69-75.

[63] Zafisah, N. S., Ang, W. L., & Mohammad, A. W. (2018). Cake Filtration for Suspended Solids Removal in Digestate from Anaerobic Digested Palm Oil Mill Effluent (POME). *Water Conservation and Managment (WCM), 2*, 5-9.

[64] Nag, A. (2016). *Distillation & Hydrocarbon Processing Practices.* Tulsa, Oklahoma: PennWell Corporation.

[65] Naeger, D. P., & Perugini, J. J. (1989). *United States of America Patent No. 4992210A.*

[66] Akvan, F., & Javaherdasthi, R. (2016). Source detection and removal of organic chloride component in crude oil. *The European Corrosion Congress* (pp. 1-7). EuroCorr 2016.

[67] ASTM International. (2019). ASTM D4929 - 19. *Standard Test Method for Determination of Organic Chloride Content in Crude Oil*. ASTM International.

[68] Dugo, G., Pellicanò, T. M., La Pera, L., Lo Turco, V., Tamborrino, A., & Clodoveo, M. L. (2007). Determination of inorganic anions in commercial seed oils and in virgin olive oils produced from de-stoned olives and traditional extraction methods, using suppressed ion exchange chromatography (IEC). *Food Chemistry, 102*, 599-605.

[69] Wai Lin, S., Kuntom, A., Ibrahim, N. A., Ramli, M. R., & Razak, R. A. (2012). the possible mitigation procedures for the reduction of the formation of chloropropanol esters and related compounds. *Palm Oil Developments, 57*, 21-27.

[70] Nagy, K., Sandoz, L., Craft, B., & Destaillats, F. (2011). Mass-defect filtering of isotope signatures to reveal the source of chlorinated palm oil contaminants. *Food Additives and Contaminants, 28*, 1492-1500.

[71] Matthäus, B., Pudel, F., Fehling, P., Vosmann, K., & Freudenstein, A. (2011). Strategies for the reduction of 3-MCPD esters and relatedcompounds in vegetable oils. *European Journal of Lipid Science and Technology, 113*, 380-386.

[72] Coker, A. K. (2010). Chapter 11 - Petroleum, Complex-Mixture Fractionation, Gas Processing, Dehydration, Hydrocarbon Absorption and Stripping: Part 2: Fractionation. In A. K. Coker, *Ludwig's Applied Process Design for Chemical and Petrochemical Plants - Volume 2: Distillation, packed towers, petroleum fractionation, gas processing and dehydration* (pp. 269-344). Gulf Professional Publishing.

[73] Ou, J. D., & Rosenfeld, D. D. (1990). *United States of America Patent No. 5107061.*

[74] Reusser, R. E. (1973). *United States of America Patent No. 3862900.*

[75] Wen, Z., Yu, X., Tu, S.-T., Yan, J., & Dahlquist, E. (2010). Biodiesel from waste cooking oil catalyzed by TiO2 - MgO mixed oxides. *Bioresource Technology, 101*, 9570-9576.

[76] *Make Biodiesel*. (2019, October 7). Retrieved from Acid Number to FFA Conversions: http://www.make-biodiesel.org/Biodiesel-Chemsitry/acid-number-to-ffa-conversions.html

[77] Ma, F., & Hanna, A. M. (1999). Biodiesel production: a review. *Bioresource Technology, 70*, 1-15.

[78] Diaz-Felix, W., R., R. M., Zimmet, W., & Kazz, M. (2009). Pretreatment of yellow grease for efficient production. *Biomass and Bioenergy, 33*, 558-563.

[79] Rogelio, S.-B., & Trejo-Zárraga, F. (2012). Hydroconversion of Triglycerides into green Liquid Fuels. In I. Karamé, *Hydrogenation* (pp. 187-216). IntechOpen.

[80] Fraser, S. (2014). Distillation in Refining. In A. Górak, & H. Schoenmakers, *Distillation: Operation and Applications* (pp. 155-190). Dortmund: Elsevier.

[81] Vogelpohl, A. (2015). The principles and modes of distillation. In A. Vogelpohl, *Distillation: The Theory* (pp. 1-4). Berlin/Boston: De Gruyter.

[82] Sorsamäki, L., & Nappa, M. (2016). *Design and selection of separation processes.* Jyväskylä/Espoo: VTT.

[83] Theodore, L., & Ricci, F. (2010). Distillation. In L. Theodore, & F. Ricci, *Mass Transfer Operations For the Practicing Engineer* (pp. 119-186). Hoboken, New Jersey: John Wiley & Sons.

[84] Lausberg, N., Josten, H., Fieg, G., Kapala, T., Cristoph, R., Sussenbach, A., . . . Schwerin, A. (2008). *United States of America Patent No. US20060006056A1.*

[85] Luyben, W. L. (2013). Analysis of Distillation Columns. In W. L. Luyben, *Distillation Design and Control Using Aspen Simulation* (pp. 61-77). American Institute of Chemical Engineers.

[86] Habibullah, A., Cumare, F. E., Sakata, M., & Hashiguchi, G. (1998). Crude Vacuum Distillation: Wet, Dry or Damp. *Petrtotech 98 Conference, Bahrain* (pp. 1-14). Pasadena: Parsons Process Group Inc.

[87] Martin, G., Lines, J., & Golden, S. (1994). Understand vacuum-system fundamentals. *Hydrocarbon Processing*, 91-98.

[88] Gupta, M. K. (2017). Deodorization. In K. G. Monoj, *Practical Guide to Vegetable Oil Processing* (pp. 217-247). Lynnwood, TX: Elsevier Inc.

[89] Hage, H. E. (2020, January 30). *Croll Reynolds Steam Ejectors*. Retrieved from Croll Reynolds Web site: https://croll.com/vacuum-systems/applications/chemical-processing/24-2/

[90] Cermak, S. C., Evangelista, R. L., & Kenar, J. A. (2012). Distillation of Natural Fatty Acids and Their Chemical Derivatives. In S. Zereshki, *Distillation - Adcvances from Modelling to Applications* (pp. 109-140). IntechOpen.

[91] Air Liquide Engineering & Construction. (2019, October 7). *Producing and processing fatty acid*. Retrieved from Air Liquide Engineering & Construction: https://www.engineering-airliquide.com/fatty-acid

[92] Erickson, D. R. (1995). Deodorization. In D. R. Erickson, *Practical Handbook of Soybean Processing and Utilization* (pp. 239-257). St. Louis, Missouri: Elsevier Inc.

[93] Hickman, K. C. (1944). High-vacuum Short-path Distillation-A Review. *Chemical Reviews, 34*, 51-106.

[94] Alasti, P., & Duncan, A. (2019, January). Removing environmental contaminants: comparing multi-stage thin-film evaporation with gas stripping and short-path distillation. *INFORM, 30*.

[95] De Greyt, W. (2013). Edible Oil Refining: Current and Future Technologies. In W. Hamm, R. J. Hamilton, & G. Calliauw, *Edible Oil Processing* (pp. 127-150). John Wiley & Sons.

[96] Xu, X., Jacobsen, C., Nielsen, N. S., Heinrich, M. T., & Zhou, D. (2002). Purification and deodorization of structured lipidsby short path distillation. *European Journal of Lipid Science and Technology, 104*, 745-755.

[97] Couper, J. R. (2019). Section 9: Process Economics. In D. W. Green, & M. Z. Southard, *Perry's Chemical Engineers' Handbook.* McGraw Hill Education.

[98] Loh, & H.P. (2002). *Process Equipment Cost Estimation Final Report.* Pittsburgh: U.S. Department of Energy.

[99] Aspen Technology. (2019). Aspen V10 built-in user guide.

[100] Suthar, K., & Joshipura, M. (2011). A comparative study on predictions of vapor liquid equilibrium of biodiesel systems. *International Conference on Current Trend in Technology, NUiCONE*, (pp. 1-6). Ahmedabad.

[101] Wittig, R., Lohmann, J., & Gmehling, J. (2003). Vapor-Liquid Equilibria by UNIFAC Group Contribution. 6. Revision and Extension. *Industrial & Engineering Chemistry Research, 42*, 183-188.

[102] 이재우, & 강래형. (2015). *South Korea Patent No. 101683392.*

[103] Chow, M., & Ho, C. (2002). Chemical composition of oil droplets from palm oil mill sludge. *Journal of Oil Palm Research, 14*, 25-34.

[104] Seefelder, W., Varga, N., Studer, A., Williamson, G., Scanlan, F., & Stadler, R. (2008). Esters of 3-chloro-1,2-propanediol (3-MCPD) in vegetable oils: Significance in the formation of 3-MCPD. *Food Additives and Contaminants*, 391-400.

[105] Adams II, T. A. (2018). *Learn Aspen Plus in 24 Hours.* McGraw Hill Education.

[106] Aspentech. (2017, January 20). *Can the shortcut distillation model DSTWU be used for non-ideal mixtures?* Retrieved from Aspentech Support Center: https://esupport.aspentech.com/S_Article?id=000083878

[107] Muzenda, E. (2013). From UNIQUAC to Modified UNIFAC Dortmund: A Discussion. *3rd International Conference on Medical Sciences and Chemical Engineering (ICMSCE'2013).* Bangkok.

[108] The Unifac Consortium. (2019, December 13). *Model Comparison*. Retrieved from The Unifac Consortium Web site: http://unifac.ddbst.de/model-comparison.html

[109] The Unifac Consortium. (2019, December 16). *UNIFAC, Modified UNIFAC (Dortmund), PSRK, VTPR*. Retrieved from The Unifac Consortium Web site: http://unifac.ddbst.de/unifac_.html

[110] Zelinková, Z., Svejkovská, B., Velísek, J., & Dolezal, M. (2006). Fatty acid esters of 3-chloropropane-1,2-diol in edible oils. *Food additives and contaminants, 23*, 1290-1298.

[111] Kister, Z. H. (1990). *Distillation Operation.* McGraw-Hill.

[112] Helmenstine, A. M. (2019, July 25). *How Does Steam Distillation Work?* Retrieved from ThoughtCo. Web site: https://www.thoughtco.com/definition-of-steam-distillation-605690

[113] Aspentech. (2017, April 10). *Getting Started with Column Analysis in Aspen Plus*. Retrieved from Aspentech Support Center: https://esupport.aspentech.com/S_Article?id=000067874

[114] Aerstin, F., & Street, G. (1978). *Applied Chemical Process Design.* New York: Plenum Press.

[115] the European Union. (2019). *Natural gas price statistics.* the European Union. Retrieved from https://ec.europa.eu/eurostat/statistics-explained/index.php/Natural_gas_price_statistics#Natural_gas_prices_for_non-household_consumers

[116] Engineering Toolbox. (2019, January 13). *Combustion Processes and Combustion Efficiency*. Retrieved from The Engineering Toolbox Web site: https://www.engineeringtoolbox.com/combustion-process-efficiency-d_1025.html

[117] Australian Government, Department of the Environment and Energy. (2019). *Factsheet, Boilet Efficiency.* Australian Government, Department of the Environment and Energy. Retrieved from https://www.energy.gov.au/sites/default/files/hvac-factsheet-boiler-efficiency.pdf

[118] Ohio University. (2019, February 13). *p-h diagram for water*. Retrieved from Ohio University Web site: https://www.ohio.edu/mechanical/thermo/property_tables/H2O/ph_water.html

[119] USA Department of Energy. (2019, January 14). *How To Calculate The True Cost of Steam*. Retrieved from USA Department of Energy Web site: https://www.energy.gov/sites/prod/files/2014/05/f15/tech_brief_true_cost.pdf

[120] Westerlund, T. (2009). *Anläggnings- och Systemteknik.* Turku: Åbo Akademi.

[121] The Engineering Toolbox. (2020, January 14). *Water - Specific Heat*. Retrieved from The Engineering Toolbox Web site: https://www.engineeringtoolbox.com/specific-heat-capacity-water-d_660.html

[122] Thulukkanam, K. (2013). *Heat Exchanger Design Handbook.* Taylor & Francis Group.